The lambeosaurine dinosaur *Amurosaurus riabinini*, from the Maastrichtian of Far Eastern Russia

PASCAL GODEFROIT, YURI L. BOLOTSKY, and JIMMY VAN ITTERBEECK

Godefroit, P., Bolotsky, Y.L., and Van Itterbeeck, J. 2004. The lambeosaurine dinosaur *Amurosaurus riabinini*, from the Maastrichtian of Far Eastern Russia. *Acta Palaeontologica Polonica* 49 (4): 585–618.

Amurosaurus riabinini Bolotsky and Kurzanov, 1991 (Dinosauria, Hadrosauridae) is described on the basis of numerous disarticulated bones from the Maastrichtian Udurchukan Formation of Blagoveschensk, Far Eastern Russia. Comparisons with North American palynozones and their well-calibrated ages suggest that this formation is late Maastrichtian in age. It is shown that *A. riabinini* is a valid species, characterised by cranial and postcranial autapomorphies. A phylogenetic analysis, based on 40 cranial, dental, and postcranial characters, indicates that this taxon occupies a relatively basal position within the lambeosaurine subfamily as the sister-taxon of a monophyletic group formed by the parasauroloph and corythosaur clades. This cladogram also demonstrates that lambeosaurines have an Asian origin. In eastern Asia, lambeosaurine dinosaurs dominate late Maastrichtian dinosaur localities, whereas this group is apparently no longer represented in synchronous localities from western North America.

Key words: Dinosauria, Lambeosaurinae, *Amurosaurus riabinini*, phylogeny, palaeogeography, Late Cretaceous, Russia.

Pascal Godefroit [pascal.godefroit@naturalsciences.be], Department of Palaeontology, Institut royal des Sciences naturelles de Belgique, rue Vautier 29, 1 000 Brussels, Belgium;
Yuri L. Bolotsky [bolotdino@tsl.ru], Amur Natural History Museum, Amur KNII FEB RAS, per. Relochny 1, 675 000 Blagoveschensk, Russia;
Jimmy Van Itterbeeck [jimmy.vanitterbeeck@geo.kuleuven.ac.be], Aspirant FWO-Vlaanderen, Afdeling Historische Geologie, Katholieke Universiteit Leuven, Redingenstraat 16, 3000 Leuven, Belgium.

Introduction

In 1902, the Russian Colonel Manakin collected isolated bones from Cossack fishermen in the vicinity of the village of Jiayin, along the Chinese bank of Amur River (named Heilongjiang, meaning Black Dragon River, in China): these were the first dinosaur fossils collected in this area (Fig. 1). During the summers 1916 and 1917, the Geological Commitee of Russia undertook two excavation campaigns at this locality. Riabinin (1925, 1930a) attested that bones belonging to hadrosaurid dinosaurs were particularly abundant at Jiayin and named two new hadrosaurid taxa from the discovered material: *Trachodon amurense* Riabinin, 1925 and *Saurolophus krystofovici* Riabinin, 1930b. Both taxa are now regarded as *nomina dubia*, because they are based on fragmentary and non-diagnostic material. Godefroit et al. (2000, 2001) reviewed part of the material that had previously been discovered at Jiayin and described a new hollow-crested—or lambeosaurine—hadrosaurid taxon: *Charonosaurus jiayinensis*.

Rozhdestvensky (1957) was the first to mention the presence of dinosaur fossils in the Russian part of the Amur region; he collected isolated and worn bones at Blagoveschensk and along the right bank of Bureya River. However, he misinterpreted the geological context of the discoveries, believing that the bones were reworked within latest Neogene or Quaternary deposits.

In 1984, Yuri L. Bolotsky and the Amur Complex Integrated Research Institute (Amur KNII) of the Far Eastern Branch of the Russian Academy of Sciences discovered a large dinosaur bonebed at Blagoveschensk. By 1991, although only a small area of about 200 square metres was excavated, several hundreds bones were recovered from this locality. Most of them belong to lambeosaurine dinosaurs. Bolotsky and Kurzanov (1991) briefly described a small part of the lambeosaurine material under the name *Amurosaurus riabinini*. Hadrosaurine hadrosaurids are also represented by cranial material (Bolotsky and Godefroit 2004). The Blagoveschensk locality has also yielded isolated teeth belonging to theropod dinosaurs (Alifanov and Bolotsky 2002).

In 1991, a third dinosaur locality was discovered in the Amur region at Kundur. Among other material, this locality has yielded the nearly complete skeleton of a new hollow-crested hadrosaurid dinosaur, *Olorotitan arharensis* Godefroit, Bolotsky, and Alifanov, 2003.

The aim of the present paper is to describe the fossil material referred to as the lambeosaurine *Amurosaurus riabinini* discovered at Blagoveschensk (Fig. 1). Until now, this discovery has gone completely unnoticed. Although it is the most abundantly known dinosaur ever discovered on the Russian territory, this taxon was even not mentioned in the most recent synthesis of ornithopod dinosaurs from Russia and Central Asia (Norman and Sues 2000).

Fig. 1. Map with the geographical location of the dinosaur localities in the Amur region (Russia) and in Heilongjiang Province (P.R. China).

Institutional abbreviations.—The described specimens are housed in the Amur Natural History Museum (abbreviated AENM) of the Amur Complex Integrated Research Institute of the Far Eastern Branch of the Russian Academy of Sciences, Blagoveschensk, Russia (abbreviated Amur KNII, FEB RAS).

Geological setting

The Blagoveschensk dinosaur locality is situated within the city limits of Blagoveschensk (Amur Region, Far Eastern Russia). The outcrops of the dinosaur site are limited to a talus a few metres high (Fig. 2). The dinosaur-bearing sediments are green-coloured claystones with a considerable amount of dispersed granules. A basal pebble lag with a maximum clast size of 20 cm occurs at the base of these sediments, The total thickness of the Cretaceous sediments in outcrop is estimated as 2–3 m. Indurated metamorphic rocks, which are weathered at the top, form the basal part of the outcrop. In outer appearance the weathered zone cannot be distinguished from the underlying rocks because the original texture of the metamorphic rocks is preserved. Only after a closer examination does it become evident that the top zone is friable and clay-rich in contrast to the indurated rocks below.

Dinosaur bones form a continuous bonebed at the base of the Cretaceous sediments. Only a small surface of about 200 m^2 has been excavated to date. Several hundreds skeletal elements were recovered from the bonebed (Fig. 3A). More than 90% of them belong to lambeosaurine dinosaurs. The skeletons are completely disarticulated and mixed. Articulation between skeletal elements is rare; only the holotype skull elements and a few series of vertebrae can be proved to belong to the same animal. Fig. 3B represents the orientation of long bones within the bonebed. Although this orientation is variable, without statistical significance, it appears that a majority of long bones have a preferred NNW–SSE orientation. Dislocation of the skeletons and preferential orientation of the long bones are indicative for deposition in fluvial or alluvial palaeoenvironment. However, considering the good state of preservation of many bones, including fragile skull elements

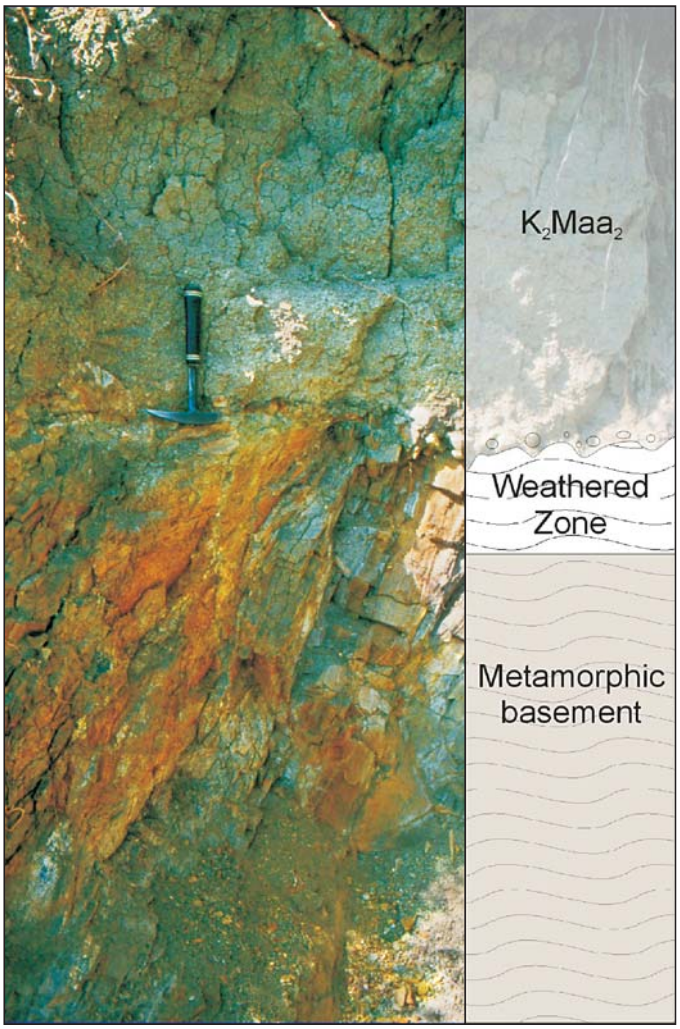

Fig. 2. Stratigraphic section of the dinosaur locality at Blagoveschensk. Abbreviation: K_2Maa_2, Udurchukan Formation (Maastrichtian).

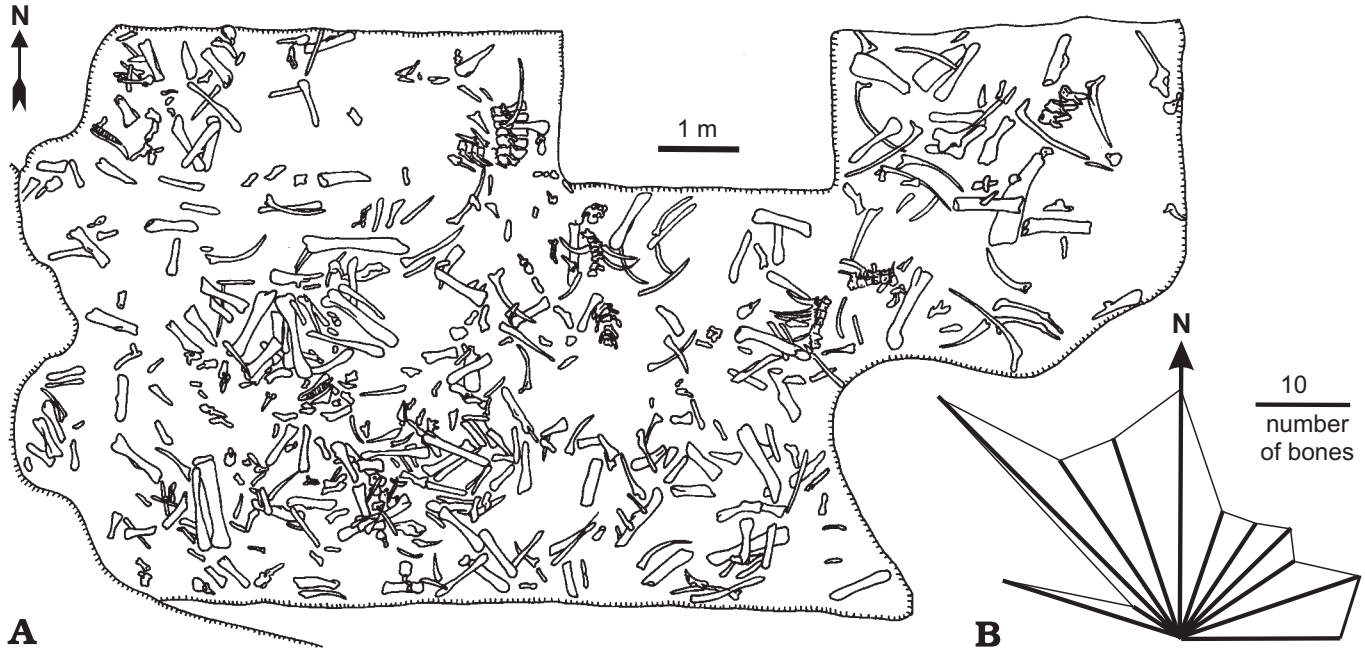

Fig. 3. **A**. Sketch showing bonebed at Blagoveschensk dinosaur locality. **B**. Diagram showing orientations of long bones at Blagoveschensk dinosaur locality.

and the apparent lack of sorting by size of the bones, fluvial transportation over a long distance seems unlikely. The abundance of theropod shed teeth and the frequency of tooth marks on the bones is indicative for an intensive activity of predators or scavengers.

The age of the Blagoveschensk dinosaur locality

The Blagoveschensk site is located in the Amur-Zeya Basin. This basin was formed as a series of N–S-trending grabens beginning in the Late Jurassic, when rifting took place over the entirety of eastern Asia (Kirillova et al. 1997). The dinosaur localities of Amur-Zeya Basin, Blagoveschensk, and Kundur were discovered in the Udurchukan Formation, which forms the lower part of the Tsagayan Group (Markevich and Bugdaeva 1997). According to Markevich and Bugdaeva (2001), this formation is correlated with the Yuliangze Formation, which has yielded abundant dinosaur material at Jiayin, along the Chinese banks of Amur River (Godefroit et al. 2000, 2001). Markevich and Bugdaeva (2001) placed the dinosaur-bearing Udurchukan Formation within the *Wodehouseia spinata–Aquilapollenites subtilis* palynozone (as defined by Markevich 1994). As such, the Russian dinosaur sites at Kundur and Blagoveschensk are dated as middle Maastrichtian (Markevich and Bugdaeva 1997). Recently, an early Maastrichtian age has been proposed for the Kundur dinosaur site (Markevich and Bugdaeva 2001). The overlying sediments of the middle part of the Tsagayan Formation, belonging to the *Orbiculopollis lucidus–Wodehouseia avita* palynozone (Markevich and Bugdaeva 2001), are dated as late Maastrichtian (Markevich 1994). Presently, no dinosaur fossils have been recovered from the middle part of the Tsagayan Group and therefore Bugdaeva et al. (2000) concluded that dinosaurs disappeared in the Russian Far East three million years before the beginning of the Cenozoic. Because of the general consensus on the extinction of dinosaurs at the K/T boundary—whether this happened gradually or catastrophically is irrelevant for the present discussion—the middle Maastrichtian age of the youngest dinosaur-bearing sediments in the Amur region is more closely examined in the following section.

The age proposed for the Russian dinosaur sites is based on the age of the palynozones to which the dinosaur-bearing sediments can be attributed. The ages of these zones are based on comparisons with other palynological assemblages in neighbouring basins (Markevich 1994). None of these age estimations of the palynozones in the Russian Far East has been calibrated by radiometric dating or palaeomagnetostratigraphy. During the Late Cretaceous, eastern Asia and western North America were part of the same microfloral province, the *Aquilapollenites* Province (Herngreen and Chlonova 1981; Herngreen et al. 1996). Therefore, a comparison of the palynozones of the Western Interior Basin with those of the Russian Far East might be instructive.

Among the angiosperm palynomorphs listed for Blagoveschensk, six are characteristic for the *Wodehouseia spinata* Assemblage Zone in the United States (Nichols and Sweet 1993; Nichols 2002): *Aquilapollenites reticulatus*, *A. quadrilobus*, *A. conatus*, *Orbiculapollis lucidus*, *Ulmipollenites krempii*, and *Wodehouseia spinata*. Those six taxa are also recorded at the Kundur dinosaur locality, together with *Proteacidites thalmanii* and *Erdtmanipollis albertensis*, other taxa characteristic for of this assemblage zone in North

Table 1. Tentative correlation of palynological zonation schemes in eastern Russia and in western North America. Abbreviations: eeEP, earliest Paleocene; eEM, early early Maastrichtian; eEP, early early Paleocene; eLM, early late Maastrichtian; lEM, late early Maastrichtian; lEP, late early Paleocene; lLM, late late Maastrichtian; mlM, middle late Maastrichtian.

Eastern Russia			North America (Canada and USA)							
Markevich 1994			Braman and Sweet 1999					Nichols 2002		
age		palynozonal scheme	age			palynozonal scheme				
Danian		*Triatriopollenites–Plicoides–Comptonia sibrica*	Paleocene	middle		*Aquilapollenites spinulosus*				
				early	lEP	*Momipites wyomingensis Tricolporollenites kruschii*				
		Wodehouseia fimbriata–Ulmoideipites krempii			eEP	*Wodehouseia fimbriata*				
Maastrichtian	late	*Orbiculapollis lucidus–Wodehouseia avita*			eeEP	*Wodehouseia spinata*	*A. reticulatus*			
	middle	*Wodehouseia spinata–Aquilapollennites subtilis*	Maastrichtian	late	lLM		*Myrtipites scabratus/ A. delicatus* var. *collaris*	*Wodehouseia spinata*	E	
					mLM				D	
	early				eLM		*Porosipollis porosus/ Aquilapollenites notable*		C	
				early	lEM				B	
									A	
							Scollardia trapaformis (*Mancicorpus gibbus* Subzone)			
					eEM		*Mancicorpus vancampoi*			

Wodehouseia spinata
Wodehouseia fimbriata
Aquilapollennites conatus
Dinosaur fossilis

America. The *Wodehouseia spinata* Assemblage Zone (Nichols 2002 and references therein) is the palynostratigraphic zone that represents the late Maastrichtian in continental rocks in western North America. It is recognised across western North America from New Mexico to the Yukon and the Northwest Territories (Nichols and Sweet 1993). The lower limit of this zone is defined by the first occurrence of *W. spinata*, the upper limit by the extinction of most taxa specific for this assemblage at the K/T boundary. The *Wodehouseia spinata* Range Zone of Braman and Sweet (1999) has a slightly different range. The lower limit of this zone is also defined by the first occurrence of *W. spinata* and coincides with the lower limit of the assemblage zone. From a biostratigraphic point of view, it starts at the top of the late early Maastrichtian. The upper limit of this zone, however, is the first occurrence of *W. fimbriata*. As a consequence the upper part of this zone falls within the early Paleocene and the extinction events at the K/T boundary fall within this zone. It was demonstrated that the Ir-anomaly at the K/T boundary falls within the *Wodehouseia spinata* Assemblage Zone in the Western Interior Basin (Nichols et al. 1986; Lerbekmo et al. 1987). As demonstrated by Nichols (2002), the Cretaceous part of the *Wodehouseia spinata* Range Zone is equivalent to the *Wodehouseia spinata* Assemblage Zone. This zone characterises well-known vertebrate-bearing strata such as the Scollard Formation in Alberta (Srivastava 1970), the Lance Formation in Wyoming (Leffingwell 1970), the Hell Creek Formation in Montana and the Dakotas (Nichols 2002), the Laramie, Arapahoe and lower part of the Denver Formations in Colorado (Newman 1987). It is equivalent to the Lancian age of vertebrate biostratigraphy (Nichols 2002). In combination with palaeomagnetic measurements and the ammonite ages of marine intercalations, this leads to a well-calibrated age for the *Wodehouseia spinata* Assemblage Zone in the Western Interior Basin, ranging from the latest early Maastrichtian to the earliest Paleocene.

The presence of *Aquilapollenites conatus* at Blagoveschensk is also interesting from a biostratigraphic point of view and speaks for a late Maastrichtian age for this dinosaur locality. Indeed, this species is restricted to the upper half of the *Wodehouseia spinata* Assemblage Zone in North Dakota (Subzones C to E; Nichols 2002) and in Alberta (Subzone VIIIa; Srivastava 1970). In Manitoba, it appears in the upper part of the *Porosipollis porosus/Aquilapollenites notabile*

Subzone of the *Wodehouseia spinata* Assemblage Zone (Braman and Sweet 1999).

In Table 1, the palynozones of the Russian Far East, with their ages as given by Markevich (1994), are correlated with the palynozones and their corresponding ages of Western Interior Basin as given by Braman and Sweet (1999) and Nichols (2002). The correlation between these palynozones is based on the range of *W. spinata*, W. *fimbriata*, *A. conatus*, and the extinction of dinosaurs. This correlation scheme is only tentative because the isochroneity of the *W. spinata*-range in Asia and North America remains to be proven by independent calibration of the Asian zones. Nichols and Sweet (1993) mentioned some diachroneity in the first occurrence of *W. spinata*: this taxon would have a younger first occurrence in Alberta than in the rest of the Western Interior Basin.

By comparison with North American palynozones and their well-calibrated ages, the presence of *Wodehouseia spinata*, together with other species of the *Wodehouseia spinata* Assemblage, in the Udurchukan Formation at Blagoveschensk and Kundur speaks for a late Maastrichtian age for the dinosaur localities from Amur Region rather than for an early to "middle" Maastrichtian age, as previously suggested by Markevich and Bugdaeva (1997, 2001). Further researches with independent calibrations of the Asian palynozones are necessary to completely clear out this discussion.

Systematic palaeontology

Dinosauria Owen, 1842
Ornithischia Seeley, 1887
Ornithopoda Marsh, 1881
Ankylopollexia Sereno, 1986
Hadrosauriformes Sereno, 1986
Hadrosauroidea Cope, 1869
Hadrosauridae Cope, 1869
Lambeosaurinae Parks, 1923

Amurosaurus Bolotsky and Kurzanov, 1991

Type species: *Amurosaurus riabinini* Bolotsky and Kurzanov, 1991.

Generic diagnosis.—See specific diagnosis (monospecific genus).

Amurosaurus riabinini Bolotsky and Kurzanov, 1991

Holotype: AEHM 1/12, associated left maxilla and dentary.

Type locality: Upper part of Nagornaia Street, west of Blagoveschensk City, Amur Region, Russia.

Type horizon: Udurchukan Formation (*Wodehouseia spinata– Aquilapollenites subtilis* palynozone), "middle"–late Maastrichtian, Late Cretaceous.

Emended specific diagnosis.—Lambeosaurine dinosaur characterised by the following autapomorphies: prominent median process between basipterygoid processes; sagittal crest particularly elevated on the caudal part of the parietal and forming a high, triangular and deeply excavated triangular process on the occipital aspect of the skull; squamosals separated from each other by this crest along their entire height; caudal process of postorbital particularly elongated, narrow, and regularly convex upwardly; prefrontal forming at least half of the width of the floor for the supracranial crest; ulna and radius sigmoidal both in lateral and in cranial views.

Skull and mandible

The following description of the skull of *Amurosaurus riabinini* is mainly based on AEHM 1/232, an incomplete, but finely preserved skull. The sutures between the differents bones forming the lateral wall of the braincase can be easily recognised, because the braincase is not fully ossified. In addition to this specimen, many disarticulated skull elements are housed in the collections of the Amur KNII. The following description will therefore bring some new information about the cranial anatomy of lambeosaurine dinosaurs. A tentative reconstruction of the skull of *Amurosaurus riabinini* is proposed in Fig. 4.

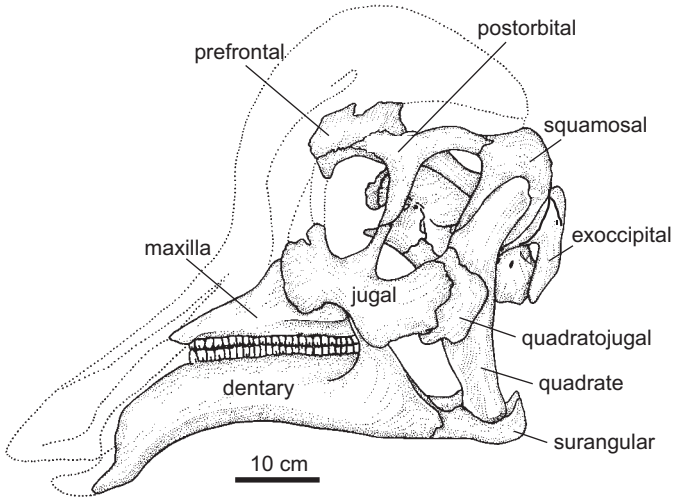

Fig. 4. Reconstruction of the skull of *Amurosaurus riabinini* in left lateral view.

The standardised anatomical nomenclature for dinosaurs recommended by Weishampel et al. (1990: fig. 6) is followed in the present paper.

Fused exoccipital-opisthotic (Figs. 5–8).—As usually observed in hadrosaurids (Horner 1992), *Iguanodon* (Norman 1980, 1986), and *Hypsilophodon* (Galton 1974), the exoccipital and opisthotic are completely fused together and there is no trace of suture between both elements. Above the foramen magnum, the caudomedian side of the exoccipital-opisthotic bears a deep, elongated and oblique sulcus in which the base of the supraoccipital inserts. Around the foramen magnum, the dorsal side of the exoccipital-opisthotic is depressed. The exoccipital condyloids are widely separated from each other by the basioccipital. The ventral base of the exoccipital condyloids is convex and rough to unite firmly

with the basioccipital. The lateral wall of the exoccipital condyloids is pierced by three foramina for transmission of cranial nerves. The caudalmost foramen is large and transmitted the hypoglossal nerve (XII). More rostrally, the foramen for the accessory nerve (XI) is the smallest of the three. The foramen for the vagus (X) and the glossopharyngeal (IX) nerves is the largest and set more dorsally than the other two. Below this latter foramen, a fourth opening is present on some specimens; it is always small and may represent a separate passage for the glossopharyngeal (IX) nerve, assumed to be the smallest of the cranial nerves. Lambe (1920) and Ostrom (1961), on the other hand, suggested that this "extra" foramen marks the emergence of the internal jugular vein; however, this hypothesis appears unlikely, because of the small size of this foramen. The foramen for IX and X is bordered rostrally by a prominent ridge extending from the ventral border of the paroccipital process to the rostroventral corner of the exoccipital condyloid. This pillar probably marks the exoccipital-opisthotic contact. In front of this ridge, the rostrodorsal corner of the exoccipital condyloid is deeply excavated by the rostral margin of the auditory foramen. From the caudal margin of the auditory foramen, a horizontal groove, which may be interpreted as a stapedial recess, runs backward along the rostral border of the prominent ridge. The paroccipital process is long and wide. As usually observed in North American hadrosaurids and in contrast to *Charonosaurus jiayinensis* (see Godefroit et al. 2000), it has a pendant aspect: its tip reaches about the level of the ventral border of the occipital condyle. In rostral view, the paroccipital process bears a wide rectangular medial facet covered by the prootic. Lateral to the supraoccipital sulcus, the paroccipital process forms a dorsal angle that inserts into a ventral depression of the squamosal in a synovial joint.

Prootic (Figs. 5, 8B).—In *Amurosaurus riabinini*, the prootic takes an important part in the formation of the lateral wall of the braincase. A broad and stout caudodorsal branch covers the rostromedial part of the fused exoccipital-opisthotic. The dorsal border of this branch also contacts the supraoccipital and parietal along a short distance. The lateral surface of the prootic bears a prominent and horizontal *crista otosphenoidalis* that extends into the rostrolateral side of the paroccipital process. The caudoventral portion of the prootic is notched by the rostral margin of the auditory foramen, whereas its rostral border is deeply excavated by the caudal margin of the large and round foramen for the trigeminal nerve (V). From this foramen, a large and deep vertical groove runs along the lateral surface of the prootic, just behind the basisphenoid process of the laterosphenoid; this ventrally-directed groove indicates the passage for *ramus mandibularis* of the trigeminal nerve (V_3). Between the notches for the auditory foramen and the trigeminal nerve, the lateral wall of the prootic is pierced by two foramina; the caudal opening transmitted *ramus hyomandibularis* of the facial nerve (VII), and the cranial foramen, *ramus palatinus* of the same nerve. A small sulcus runs from the latter foramen ventrally along the lateral side of the prootic to the vicinity of the Vidian canal; this channel housed *ramus palatinus* of the facial nerve. Above the foramen for the trigeminal nerve, the prootic process of the laterosphenoid broadly covers the lateral side of the prootic. The prootic forms also a ventrally-directed flange that extends downwardly to meet the lateral surface of the basisphenoid. A prominent ridge runs along its lateral surface, in continuity with the caudal border of the alar process of the basisphenoid, to conceal the dorsal part of the Vidian canal. The basisphenoid process of the laterosphenoid covers the rostrodorsal portion of this ventral flange.

Laterosphenoid (Figs. 5, 7B, 8B).—As is usual in hadrosaurids, the laterosphenoid of *Amurosaurus riabinini* is a stout bone bearing three processes. The prootic process forms a wide, triangular and caudally-directed wing. Both its dorsal and ventral borders are particularly broad and rough for contact respectively with the parietal and the prootic. At the junction between the laterosphenoid, parietal and prootic, a small foramen represents the passage for *vena parietalis*. The basisphenoid process forms a ventrally-directed foot that covers the alar process of the basisphenoid and the rostrodorsal part of the ventral flange of the prootic. The angle between the prootic and the basisphenoid processes forms the rostral margin of the foramen for the trigeminal foramen. From this notch, a wide and deep groove runs rostrally along the lateral side of the laterosphenoid, indicating the forward passage of the deep *ramus ophthalmicus* of the trigeminal nerve (V_1). The rostral border of the basisphenoid process is notched by an elongated foramen for the occulomotor (III) and abducens (VI) nerves. The postorbital process of the laterosphenoid is elongated and stout. It extends rostrolaterally so that its ball-like distal end abuts into a socket between the medial and ventral rami of the postorbital. From the tip of the postorbital process to the basisphenoid process, the lateral side of the laterosphenoid bears a regularly round crest marking the separation between the orbit and the supratemporal fenestra. The rostroventral border of the postorbital process forms a broad and rough surface for contact with the ventral surface of the frontal. Between this frontal facet and the notch for III and VI, a shorter but also broad and rough surface can be interpreted as a contact facet for the orbitosphenoid.

Orbitosphenoid (Figs. 5D, 6B, 7B).—This round bone participates in the rostral part of the lateral wall of the braincase and in the greatest part of the incomplete interorbital septum. Its dorsal border contacts the frontal, its caudal border the laterosphenoid, its ventral border the parasphenoid, and its rostral border the presphenoid. A small foramen for the trochlear nerve (IV) is located between the parasphenoid and the orbitosphenoid, at the caudoventral corner of the latter.

Presphenoid (Figs. 5, 7B).—The paired presphenoids form the rostral part of the interorbital septum and circumscribe the large median opening for the olfactory nerve (I). They contact dorsally the frontals.

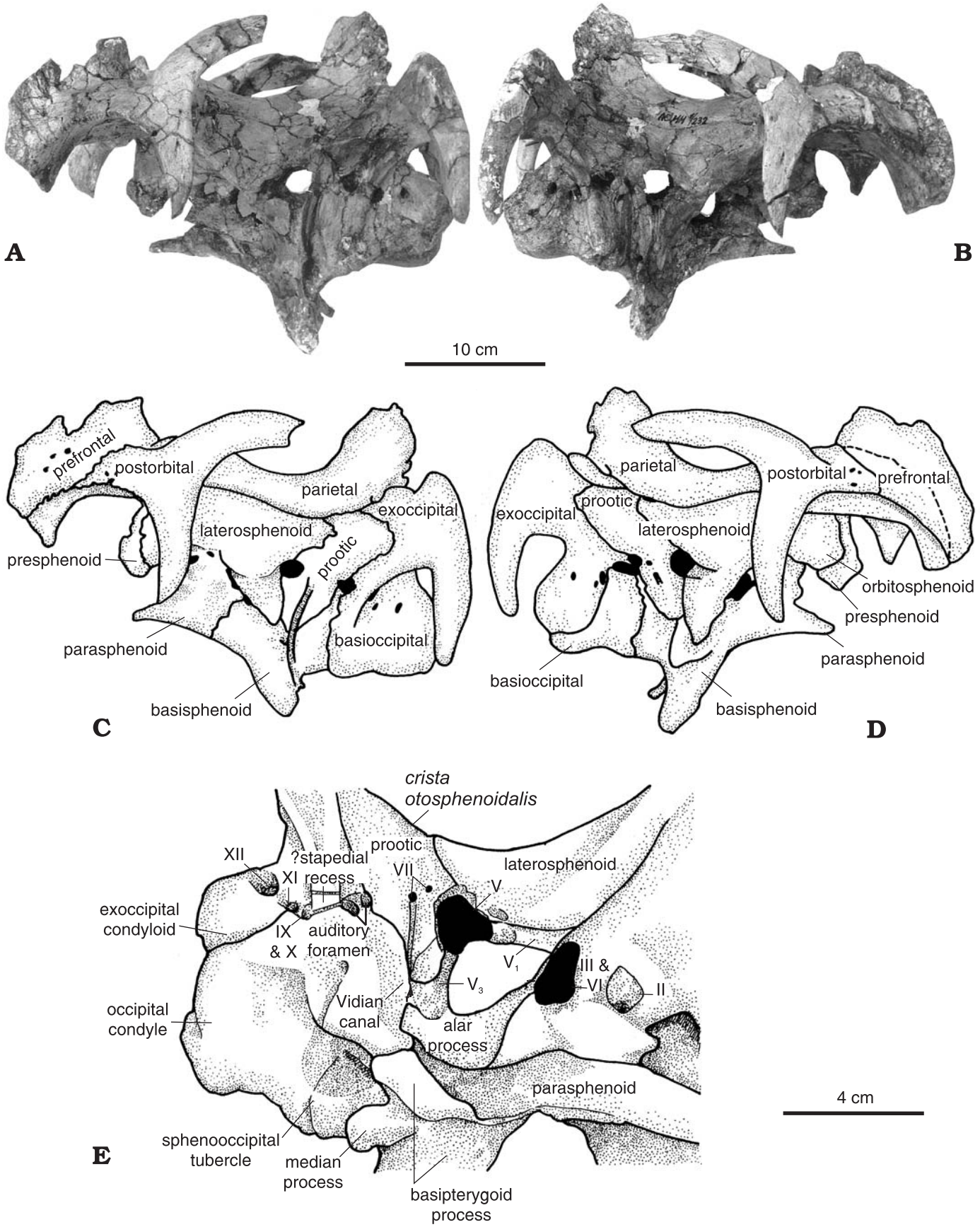

Fig. 5. Braincase of *Amurosaurus riabinini* (AEHM 1/232) in left (**A**, **C**) and right (**B**, **D**) lateral views. **E**. Detail of the right side of the braincase.

Basioccipital (Figs. 5, 7, 8B).—The basioccipital of *Amurosaurus riabinini* is distinctly wider than long. The occipital condyle is particularly broad and low. As usual in hadrosaurids, its articular surface is perfectly vertical, perpendicular to the braincase, and it is incised by a vertical furrow. The median part of the dorsal surface of the basioccipital takes a large part in the formation of the foramen magnum. The sphenooccipital tubercles are not separated from the occipital condyle by a distinct neck. They bear a lateral crest in continuity with the pilllar marking the hypothetic separation between the exoccipital and the opisthotic. In front of the large articular surface for the exoccipital condyloid, the dorsal side of the basioccipital forms a majority of the ventral margin of the auditory foramen.

Basisphenoid (Figs. 5D, 8).—Two large caudal processes, projecting slightly laterally from the basisphenoid and separated by a narrow, but deep incision, form the rostral half of the sphenooccipital tubercles. Both articular surfaces for the basioccipital are ovoid in outline and cup-shaped, facing slightly medially and ventrally. In lateral view, the caudodorsal corner of these tubercles participates in the formation of the ventral margin of the auditory foramen. The basipterygoid processes diverge from the base of the basisphenoid at an angle of about 45° from the horizontal. Their round ends therefore extend low under the level of the occipital condyle, as is usual in Hadrosauroidea. A large, but thin median process projects caudoventrally from the caudal junction between both basipterygoid processes. Such a process is also developed in *Ouranosaurus nigeriensis* (see Taquet 1976: fig. 12) and *Bactrosaurus johnsoni* (see Godefroit et al. 1998: fig. 6); with the exception of *Edmontosaurus* (see Lambe 1920: fig. 5), it has never been described in other hadrosaurids to date. Just behind the median process, the ventral surface of the basisphenoid is pierced by a small median foramen. Above the basipterygoid process and under the foramen for the trigeminal nerve, the lateral side of the basisphenoid forms a large asymmetrical alar process. The caudal part of this process conceals the Vidian canal, which carried the internal carotid artery through the basisphenoid into the hypophyseal cavity. Two other pairs of foramina pierce the caudodorsal wall of the hypophyseal cavity. The ventral openings, which correspond to the passages for the abducens nerves (VI), are the larger; they caudodorsally perforate the body of the basisphenoid to open between the large openings for the trigeminal nerves. The other two smaller paired foramina, interpreted as passages for *ramus caudalis* of the internal carotid artery, follow a similar way: they penetrate caudodorsally the wall of the hypophyseal cavity to open, as a single median foramen, between the dorsal foramina for the abducens nerves.

Parasphenoid (Figs. 5, 6B, 7B).—This bone extends forwardly and upwardly as a thin, tapering contraction of the basisphenoid, to which it is completely fused. The caudal part of the parasphenoid contacts the overlying orbitosphenoid, whereas the remainder of the bone projects freely between the orbits. It participates in the formation of the margin of three foramina for cranial nerves. Caudally, it forms the ventral margin of the large common openings for the occulomotor (III) and abducens (VI) nerves. More rostrally, it entirely surrounds the foramen for the optic nerve (II). Dorsal to the latter, it also forms the greatest part of the margin of the small foramen for the trochlear nerve (IV). The caudal part of the parasphenoid forms a shallow canal, in continuity with the hypophyseal cavity.

Supraoccipital (Fig. 7D).—The supraoccipital is a stout pyramidal bone that extends upwardly and forwardly above the occipital region. Its straight base is strongly inserted between the dorsomedial borders of the paired paroccipital processes. The dorsal surface of the supraoccipital is strongly sculptured, as usually described in hadrosaurids. Deeply depressed areas for insertion of *M. spinalis capitis* and *M. rectis capitis posterior* surround a prominent median promontorium laterally and ventrally. Lateral to these depressed areas, the caudolateral corners of the supraoccipital are formed by a pair of prominent knobs that articulate with the medioventral corner of the median rami of the squamosals and the notched caudoventral corners of the parietal. Above the knobs, the dorsal surface of the supraoccipital bears a pair of rectangular flat facets that articulate with the ventral borders of the overhanging parietal. In ventral view, the rostrodorsal part of the supraoccipital forms a large and deep depression that roofed the caudal portion of the myencephalon. The lateral sides of the supraoccipital are broad and rough for strong attachment with the adjacent bones: the paroccipital processes caudoventrally and the prootic, more rostrodorsally.

Parietal (Figs. 5, 6D, 7D).—Although it looks relatively more elongate than in other members of the subfamily, the proportions of the parietal of *Amurosaurus riabinini* are those usually observed in typical lambeosaurines: the width of the proximal end is greater than the length and the ratio "length/minimal width" < 2. The parietal contacts the frontals at the level of the rostral margin of the supratemporal fenestra in a digitate transverse suture. A short rostromedian process is interposed between the paired frontals: within lambeosaurines, such interposition has been described in *Lambeosaurus* (Gilmore 1924a), but has not been observed in *Corythosaurus* (Ostrom 1961). Paired rostrolateral processes extend laterally to contact the postorbitals. Ventrally, the parietal forms a long and straight suture with the laterosphenoid. As described by Lambe (1920) in *Edmontosaurus*, the caudoventral border of the parietal clearly contacts the prootic. The caudoventral corners of the parietal form deep notches that partly cover the supraoccipital knobs. The dorsal aspect of the parietal of *Amurosaurus riabinini* resembles that of *Corythosaurus casuarius*. The rostral part is flat; from the middle part of the bone, a strong sagittal crest rises backwardly, reaching caudally to the supratemporal arch. At the level of the sagittal crest, the lateral surfaces of the parietal, which form the medial walls of the supratemporal fenestrae, are moderatly concave both vertically and horizontally, as described in *Corythosaurus casuarius* (Ostrom 1961). On

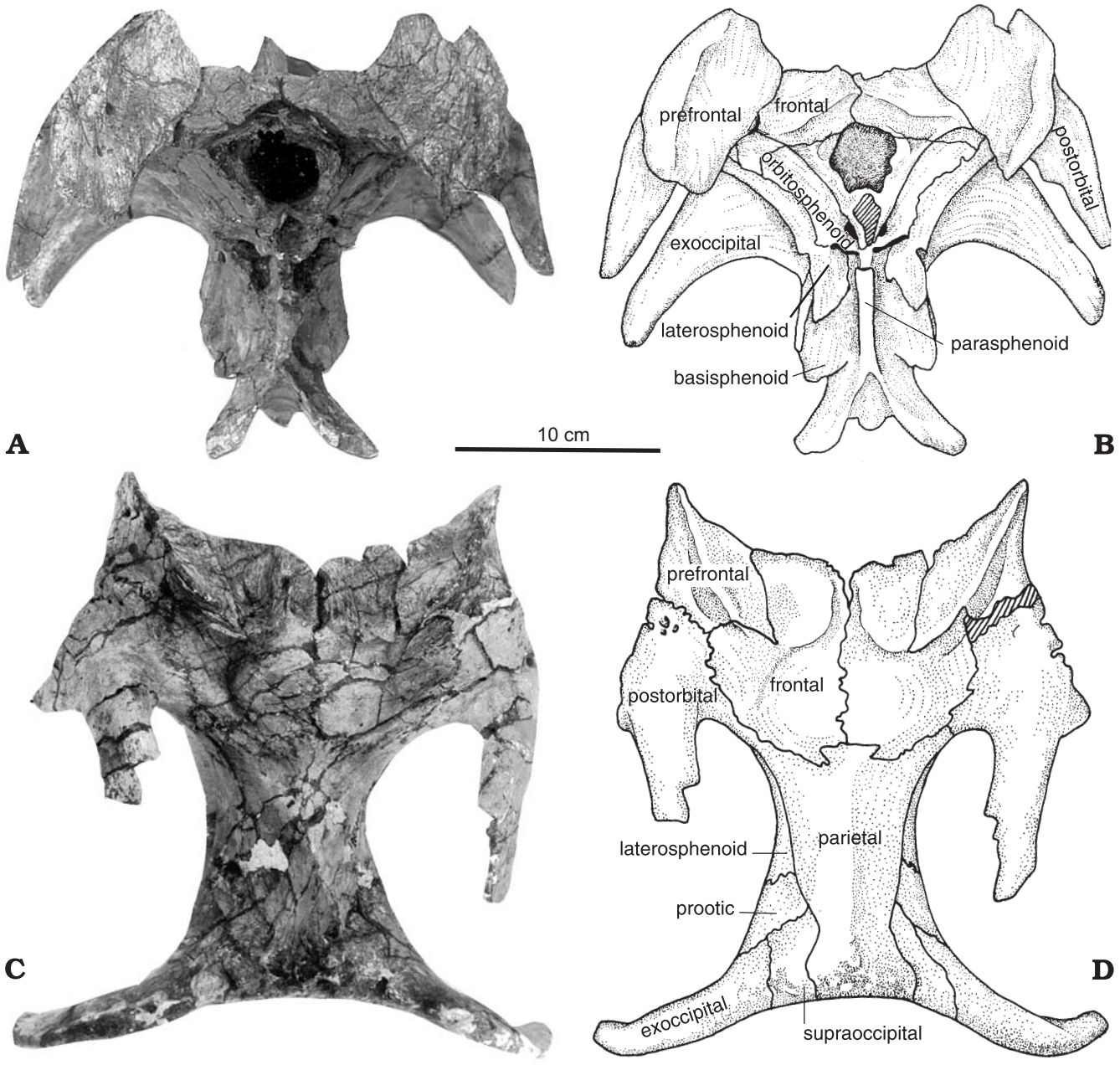

Fig. 6. Braincase of *Amurosaurus riabinini* (AEHM 1/232) in rostral (**A**, **B**) and dorsal (**C**, **D**) views.

the other hand, the caudal aspect of the parietal is completely different in *Amurosaurus* and *Corythosaurus*. In the former, the parietal forms a high triangular process that overhangs the rostrodorsal part of the supraoccipital and separates the squamosals from each other along their entire height. Elongate, rough, and caudodorsally-facing squamosal facets run along the entire caudal surface of the parietal. Because of the triangular shape of the caudal parietal process, the squamosals are better separated from each other ventrally than dorsally. The triangular caudal surface of the parietal is deeply excavated, especially in its ventral part. This depressed area may have served as attachment area for a powerful *ligamentum nuchae*. The relationships between parietal and squamosals in the occiput area are different in *Corythosaurus*. In this genus, the parietal forms a broad caudal extension comprising nearly the entire caudal wall of the supraoccipital fenestra and restricting the squamosals to the lateral walls of these openings; the squamosals meet at the midline dorsal to the supraoccipital (Ostrom 1961: fig. 54). In *Lambeosaurus* (see Gilmore 1924a), *Hypacrosaurus* (see Gilmore 1937: fig. 30; Horner and Currie 1994) and *Tsintaosaurus* (see Young 1958: fig. 1), the parietal is interposed between the paired squamosals on the occipital aspect of the skull, but does not form such a prominent caudal process as observed in *Amurosaurus riabinini.* In *Parasaurolophus* (see Sullivan and Williamson 1999: fig. 9e) and *Charonosaurus* (see Godefroit

et al. 2001), the parietal is completely excluded from the occipital surface by the squamosals.

Frontal (Figs. 5, 6, 7B).—In AEHM 1/232, as in other juvenile specimens, the frontals remain separated; in larger, thus older, specimens both elements are completely fused together. The frontals of *Amurosaurus riabinini* are relatively short, wide and thick, although remaing distinctly longer than wide. They caudally form a broad interdigitate suture with the parietal; a caudomedial notch allows the rostral process of the parietal to insert between the frontals. The caudolateral border of the frontal forms a long, particularly thick and rough articular facet for the postorbital. The dorsal surface of the frontal is highly modified to form the base of the hollow crest. Its rostral half provides a broad and strongly grooved platform that slopes forward and maximizes the area for strong attachment of the nasals and premaxillae. Lateral to the rostral platform, the frontal forms a broad, elongate, and dorsolaterally-facing contact for the prefrontal. Ontogenetic trends consist in an increase in the size of the rostral platform, both in length and in width. However, it is always narrower than the caudal part of the bone, even in larger specimens. This is also the case in *Jaxartosaurus aralensis*. In adult specimens of *Corythosaurus casuarius*, on the other hand, the rostral platform is wider than the caudal part of the frontal. Both parts have approximately the same width in the fragmentary lambeosaurine skull described by Gilmore (1937: fig. 32), from the Two Medicine Formation of Montana (?*Hypacrosaurus*). In AEHM 1/232 and in smaller specimens, the caudal half of the frontals form a median squamous doming, as usually observed in juvenile lambeosaurines. Lateral to this doming, the dorsal surface of the frontal is slightly depressed. The rostral border of the frontal forms a median hemispherical notch that might represent the dorsal passage of the respiratory tracts into the skull. This structure is probably derived from the fronto-nasal fontanelle observed in a series of juvenile hadrosaurines and non-hadrosaurid Hadrosauroidea (Maryańska and Osmólska 1979; Godefroit et al. 1998). Several cephalic impressions can be recognised on the ventral side of the frontal. On the caudal half, the impression for the cerebrum is ovoid and particularly large and deep. This area is limited laterally and rostrally by a low wall of rugosities for contact with the orbitosphenoid. Lateral to this area, the thinner ventral side of the frontal participates in the roof of the orbit. Under the rostral platform, the ventral surface of the frontal is also depressed by the impression for the olfactory lobe of the brain.

Prefrontal (Figs. 5, 6, 7B).—The dorsal aspect of the prefrontal is also highly modified to support the base of the hollow crest. It forms a long and wide dorsal platform, in continuity with the rostral frontal platform. The prefrontal platform faces inwardly and forwardly; it is concave both rostro-caudally and medio-laterally and also bears strong longitudinal grooves and ridges. Caudally, it slightly overhangs the caudolateral part of the frontal. The lateral side of the prefrontal is convex and progressively thickens caudally. Caudolaterally, it forms a broad contact surface for the postorbital. In AEHM 1/232 and in juvenile specimens, a series of more or less interconnected foramina surround the thickened part of the lateral side of the prefrontal, around the orbital rim. According to Maryańska and Osmólska (1979), this line may mark the boundary between the partially fused "true" prefrontal and supraorbital I. Both bones are completely fused in larger specimens. The lateral orbital rim is always deeply furrowed, confirming the hypothesis that this portion is really a supraorbital. The morphology of the prefrontal is different in *Amurosaurus* and *Corythosaurus*. In adult specimens of the latter genus, the frontal forms the greatest part of the platform that forms the base of the hollow crest, whereas the prefrontal participates only in the lateral aspect of the crest (Ostrom 1961). Such condition is also observed in the fragmentary lambeosaurine skull described by Gilmore (1937: fig. 33) from the Two Medicine Formation of Montana (?*Hypacrosaurus*). In *Amurosaurus*, on the other hand, the prefrontal takes an important part in the formation of the floor of the hollow crest, forming at least half the width of the basal platform. This important participation of the prefrontal in the formation of the base of the supracranial crest is also observed in *Jaxartosaurus aralensis* (see below).

Postorbital (Figs. 5, 6, 7B).—As is usual in hadrosaurids, the postorbital is a triradiate bone formed by a medial, a caudal, and a ventral ramus oriented at about 90° from each other. The medial ramus is short and particularly stout. Its medial border is thick and persillate: rostrally, it contacts the prefrontal and more caudally, the frontal. Its caudomedial corner contacts the parietal. The morphology of the caudal ramus is diagnostic for *Amurosaurus riabinini*, being different from all currently described lambeosaurines: it is particularly elongated, narrow, and regularly convex upwardly. A slight, but distinct swelling, as also observed in *Corythosaurus casuarius*, marks its basal contact with the medial ramus. On its medial side, a wide and elongated groove that progressively deepens rostrally marks the contact with the rostral ramus of the squamosal. In *Corythosaurus casuarius*, the caudal ramus of the postorbital appears more robust and less curved upwardly. In species of *Parasaurolophus*, *Tsintaosaurus spinorhinus* and *Jaxartosaurus aralensis*, it is particularly short and broad. In *Charonosaurus jiayinensis*, it is much higher and straight. The ventral ramus is triangular in cross-section and regularly curved forwardly. Its caudomedial side forms a large concave area for articulation with the ascending process of the jugal. Its lateral side is pierced by several vascular foramina. The internal orbital surface of the postorbital is concave. At the junction between the three rami, a large pocket-like depression receives the postorbital process of the laterosphenoid in a synovial joint (Weishampel 1984). In AEHM 1/232, the dorsolateral orbital rim of the postorbital is rugose and circumscribed by a series of foramina, as also observed on the prefrontal. According to Maryańska and Osmólska (1979), this feature suggests that the hadrosaurid postorbital results from the fusion of the "true" postorbital with a small supraorbital II.

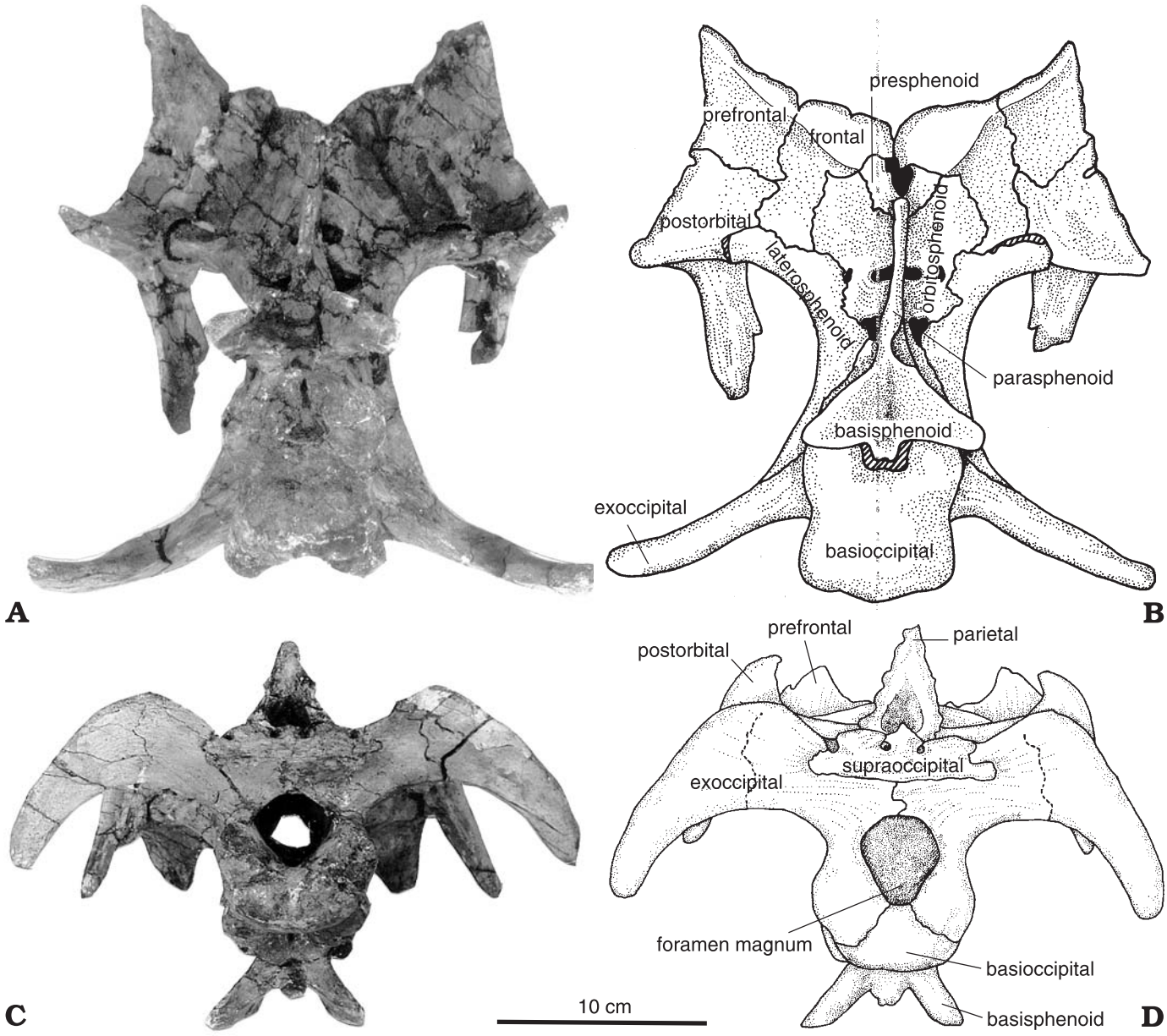

Fig. 7. Braincase of *Amurosaurus riabinini* (AEHM 1/232) in ventral (**A**, **B**) and caudal (**C**, **D**) views.

Squamosal (Fig. 9B).—The medial ramus of the squamosal is particularly elevated; its medial articular facet is thick and rough for contact with the caudal triangular process of the parietal. As discussed above, the median rami of the paired squamosals are separated from each other along their entire height. The ventromedial corner of the medial ramus forms a cup-shaped articular surface for synovial articulation with the prominent dorsal knobs of the supraoccipital. The rostral process of the squamosal is relatively slender and tapers rostrally. Its lateral side bears two strong, parallel, and ventrally-deflected longitudinal ridges that limit a long and wide articular surface for the caudal ramus of the postorbital. The lower ridge also forms the dorsal limit of a large triangular scar for attachment of *M. adductor mandibulae externus superficialis* (see Ostrom 1961: fig. 34). The precotyloid process is short, triangular in cross-section, and pointed at its distal end; it extends rostroventrally at a 45° angle. The postcotyloid process is particularly long and flat; it is less distinctly inclined rostroventrally than the precotyloid process. Its long axis is oblique so that its lateral side faces rostrally. An elongated groove runs along the caudolateral border of the postcotyloid process for reception of the lateral border of the paroccipital process. The angle between the postcotyloid process and the medial ramus of the squamosal is slightly excavated for reception of the dorsal angle of the paroccipital process. The caudolateral border of the postcotyloid process and the lateral border of the precotyloid process form a continuous ridge that laterally limits the deeply excavated

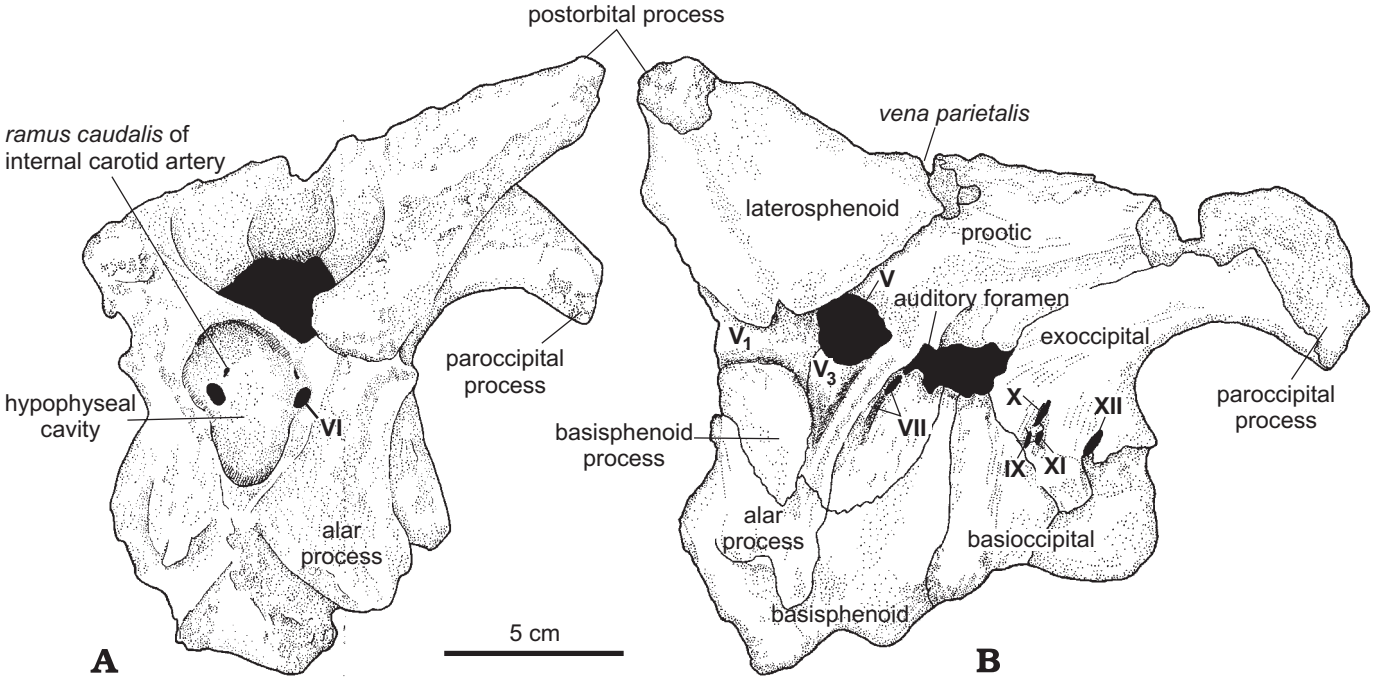

Fig. 8. Braincase of *Amurosaurus riabinini* (AEHM 1/90) in rostral (**A**) and left lateral (**B**) views.

cotylus; another continuous ridge, formed by the rostromedial border of the postcotyloid process and the caudal border of the precotyloid process, medially limits the cotylus. The body of the squamosal is elevated above the cotylus, as usually observed in lambeosaurines. The inner side of the squamosal, that forms the caudolateral margin of the supratemporal fenetra, is gently inclined inwardly and upwardly. This side bears an oblique crest running from the precotyloid process to dorsomedial corner of the medial ramus; this crest forms the ventral limit of a large scar for attachment of a powerful *M. adductor mandibulae externus medialis* (see Ostrom 1961: fig. 36).

Quadrate (Fig. 9C).—The quadrate of *Amurosaurus riabinini* is high, slender, and distinctly curved backwardly; the round proximal head is subtriangular in cross-section and flat medio-laterally. The thin pterygoid wing is always broken off on the studied material. It is oriented an angle of about 45° with the jugal wing. A prominent vertical ridge along the caudomedial side of the quadrate shaft marks the contact with the ventral quadrate process of the pterygoid. The jugal wing is regularly round and slightly curved inwardly. Beneath the jugal wing, the quadratojugal notch is high and deep. An elongated facet runs along nearly its entire height, indicating that the notch was completely covered by the quadratojugal and that the paraquadratic foramen was closed, as is usual in hadrosaurids. The distal end of the quadrate forms a large hemispherical lateral condyle that articulated with the surangular component of the mandibular glenoid. A smaller medial condyle, which fits into the articular component of the mandibular glenoid, is set more dorsally at the base of the pterygoid wing.

Jugal (Fig. 9A).—In lateral view, the rostral process is round and symmetrically expanded dorso-ventrally, with a high lacrimal process. On the medial side of the lacrimal process, the maxillary facet is particularly wide and strongly striated for tight ligamentous attachment with the maxilla. The maxillary facet is bordered caudally by a crescent-shaped and elevated maxillary process whose dorsal side bears a dorsoventrally-elongated palatine facet. Because of the important expansion of the rostral process, the jugal neck appears strongly contracted, and the ventral margin of the bone, particularly concave. The postorbital process is triangular in cross-section, slender and inclined backwardly, forming a 45° angle with the long axis of the jugal. Its rostral side is concave for reception of the ventral process of the postorbital. The caudal process of the jugal is a broad plate that rises caudodorsally at about the same angle as the postorbital process. Its ventral border is slightly concave. Its caudomedial side bears a smooth articular facet for the quadratojugal. The angle between the caudal process and the ventral border of the jugal is slightly expanded and in life would have extended over the coronoid process of the dentary.

Quadratojugal.—One partial left quadratojugal is preserved in the Blagoveschensk collection. It is a thin bone, thinner rostrally than caudally. Its lateral side is smoothly convex both rostro-caudally and dorso-ventrally. An extended smooth rostrolateral surface indicates that it was extensively overlapped by the jugal. The caudomedial side forms a large crescent-shaped concave surface where it contacted the edges of the quadratojugal notch of the quadrate. Under this surface, the caudoventral corner of the quadratojugal is truncated.

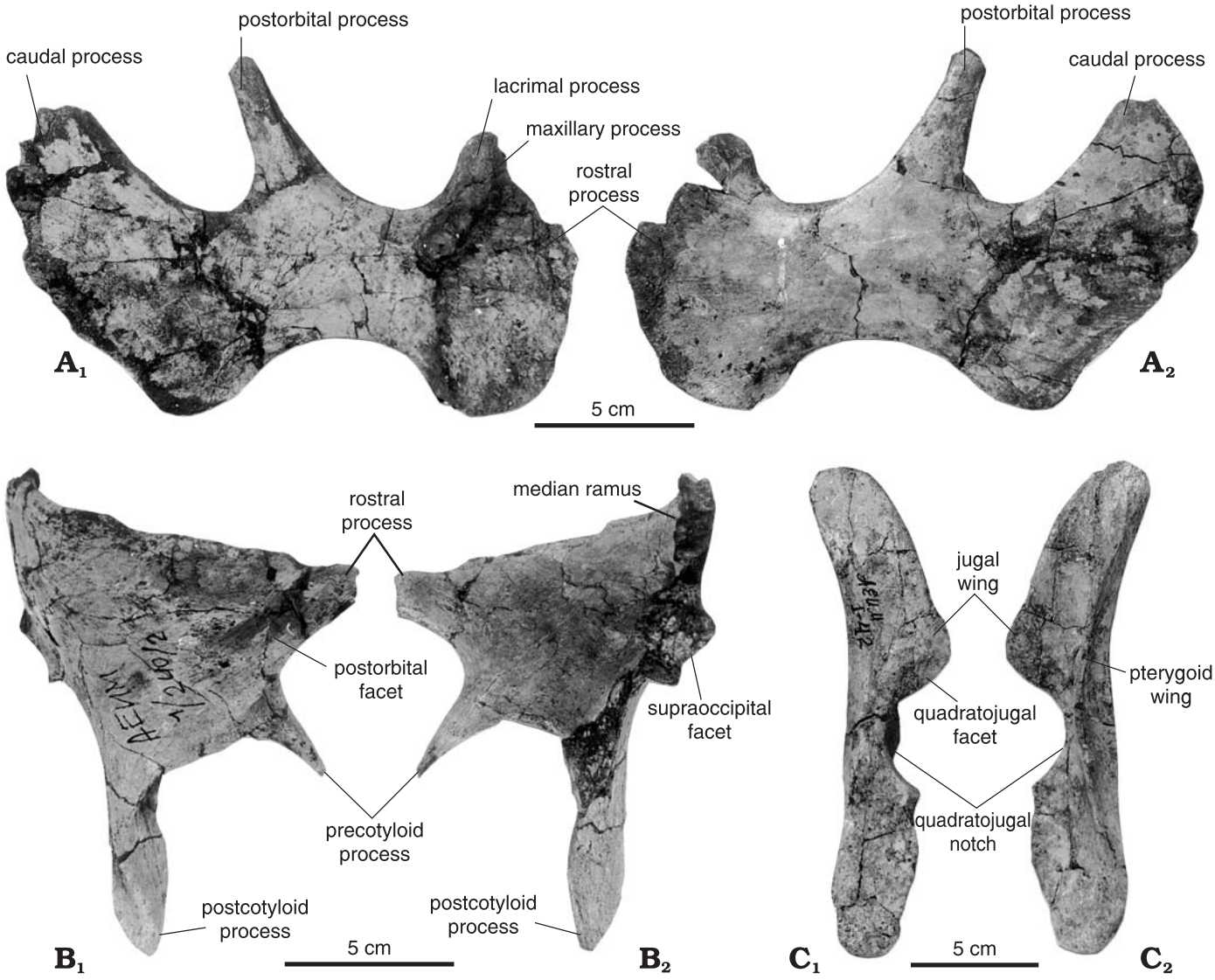

Fig. 9. *Amurosaurus riabinini*. **A**. Left jugal (AEHM 1/112) in medial (A_1) and lateral (A_2) views. **B**. Right squamosal (AEHM 1/240) in lateral (B_1) and medial (B_2) views. **C**. Right quadrate (AEHM 1/42) in lateral (C_1) and medial (C_2) views.

Maxilla (Fig. 10).—Several well-preserved maxillae are known from the Blagoveschensk collection. In lateral view, they are elevated, about twice longer than high. The dorsal process is high, triangular, and medio-laterally compressed; its caudal border is perpendicular to the base of the maxilla. Its apex lies about 20% behind the mid-point of the element so that the maxilla looks asymmetrical in lateral view. A deep elongate groove along the rostrolateral side of the dorsal process marks the contact with the lacrimal. At the base of the lacrimal facet, a large ovoid canal penetrates the dorsal process to communicate with the excavated caudomedial surface of this process; this canal has been argued to represent the antorbital fenestra among hadrosaurids (Weishampel and Horner 1990). Beneath the dorsal process, the lateral side of the maxilla forms a prominent jugal process, slightly inclined dorsally and caudally. Two oblique ridges run along the caudoventral part of the jugal process to receive the maxillary process of the jugal. Ventral to the jugal process, three to four foramina penetrate the maxilla; they run caudodorsally to open into the excavated caudomedial surface of the dorsal process behind the antorbital foramen. Behind the jugal process, a prominent, round and horizontal ridge extends caudally along the lateral surface of the maxilla and separates the ectopterygoid shelf from the dental battery. The ectopterygoid shelf is broad, dorso-ventrally concave and rostro-caudally undulating. Caudal to the dorsal process, it forms a triangular palatine process that slopes inwardly and whose caudal border bears a distinct articular facet for the palatine. More caudally, the medial edge of the ectopterygoid shelf forms a smaller triangular pterygoid process, which received the maxillary process of the pterygoid. At the caudal end of the ectopterygoid shelf, a grooved and pitted surface contacts the caudal end of the ectopterygoid. Rostral to the dorsal process, the dorsal border of the maxilla widens to form a concave shelf and a round medial

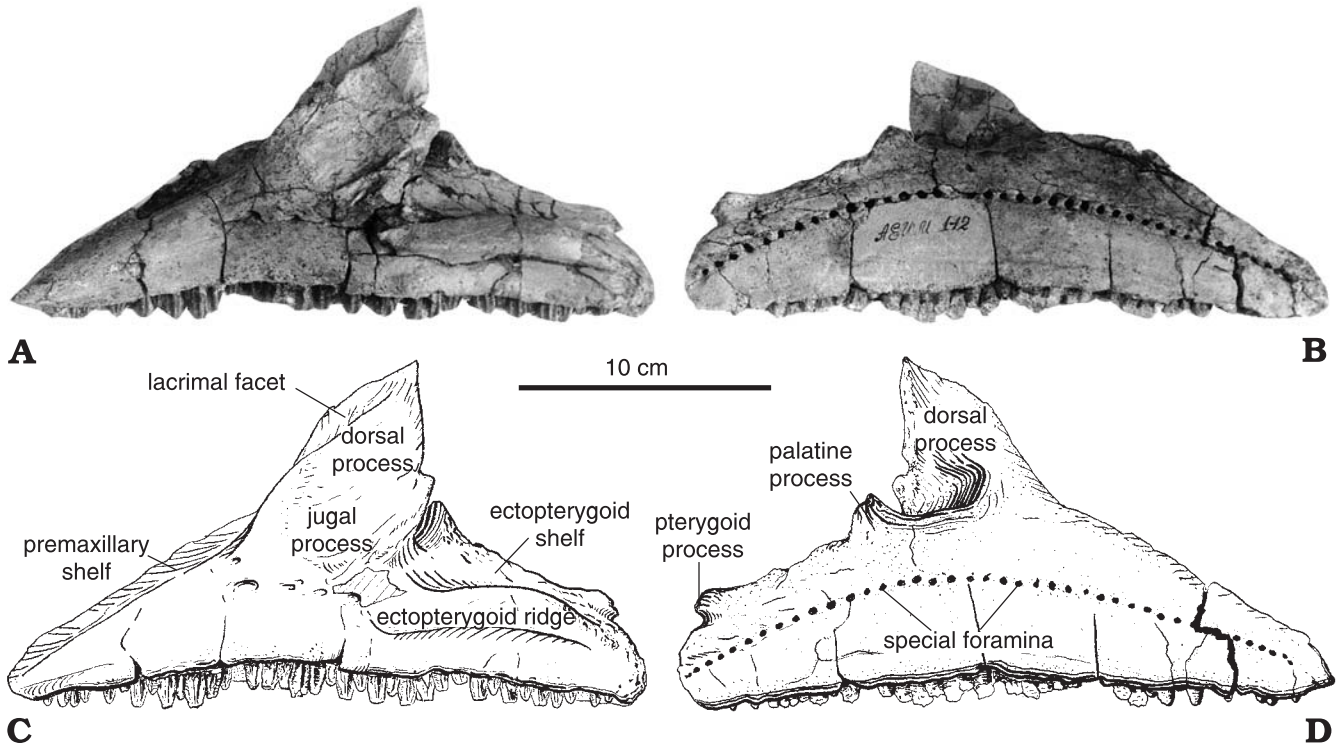

Fig 10. Left maxilla of *Amurosaurus riabinini* (AEHM 1/12) in lateral (**A**, **C**) and medial (**B**, **D**) views.

flange along which the premaxilla rested. The maxilla regularly tapers rostrally. The medial surface of the maxilla is perfectly flat and pierced by a series of special foramina interconnected by a gently curving horizontal groove, along the entire length of the bone. The number of special foramina corresponds to the number of tooth columns and each varies in size according to the size of the maxilla (about 39 in the holotype AEHM 1/12.).

Pterygoid.—One fragmentary piece of bone is interpreted here as the central part of a right pterygoid. Its caudomedial surface forms a triradiate ridge, marking the origin of three main processes: the rostral palatine process and the rostroventral ectopterygoid process run medially, whereas the ventral quadrate process runs caudolaterally. The palatine and ectopterygoid processes surround a depressed palatal arch, facing rostroventrally and medially. Between the palatine and quadrate processes, the quadrate ramus was thin, but completely broken off. This ramus would have contacted the pterygoid wing of the quadrate and abuted against the caudomedial side of the quadrate shaft.

Dentary (Fig. 11).—In this section, we describe AEHM 1/12, the holotype of *Amurosaurus riabinini*, which is the best preserved and only dentulous dentary discovered at Blagoveschensk to date. This dentary has a typical lambeosaurine design: its rostral portion is strongly deflected ventrally, forming an angle of about 30° with the long axis of the bone. The ventral deflection begins slightly rostral to the middle of the dental battery. Bolotsky and Kurzanov (1991) regarded this as a diagnostic character for the species. However, the ventral deflection is less important in smaller specimens and starts sometimes more rostrally: therefore, it may be regarded as an ontogenetic character instead. The diastema is half as long as the dental battery in the holotype, but is proportionally shorter in smaller specimens. The rostral articular surface for the predentary is typically scoop-shaped and slightly inclined to the sagittal axis of the mandible. In dorsal view, the dentary appears less curved externally than that of *Corythosaurus "excavatus"* (see Sternberg 1935: pl. 2: 1), or *Charonosaurus jiayinensis*, for examples. The lateral side of the dentary is convex dorso-ventrally. It is irregularly pierced by a series of foramina for vessels and nerves. The coronoid process is high and robust, with a flat inner side. As is usual in hadrosaurids, it slopes forwardly and is slightly curved inwardly; its lateral side bears an extended triangular surface along its dorsal part, marking the insertion of a powerful *M. pseudotemporalis*. In caudal view, the dentary is excavated by the large adductor fossa, which extends to the level of the 19th tooth row as a deep mandibular groove. Under this groove, the medial side of the dentary bears a long angular facet. The caudoventral end of the coronoid process bears a large triangular facet for the splenial. In the holotype, about 37 vertical tooth columns form the dental battery. Four or five teeth, with two effective ones, form each vertical column. Tooth replacement is the normal one illustrated by Ostrom (1961: fig. 20): distal teeth are progressively more completely erupted. The sequence of tooth eruption is therefore from back to front, with alternate rows subject to the same replacement cycle. A thin bony plate conceals the dental battery. Its base is pierced by a

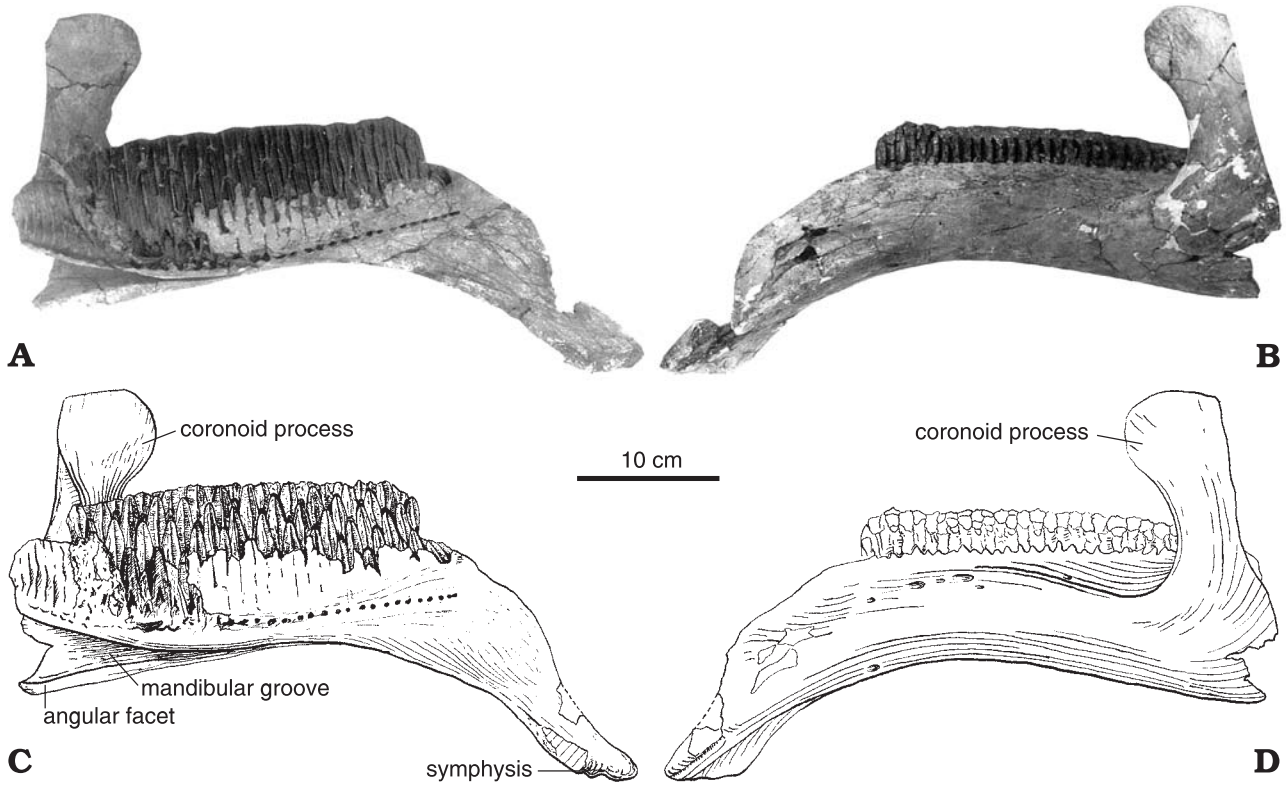

Fig. 11. Left dentary of *Amurosaurus riabininini* (AEHM 1/12) in medial (**A**, **C**) and lateral (**B**, **D**) views.

series of special foramina arranged into a horizontal line. Each foramen strictly corresponds to one tooth row.

Surangular.—In dorsal view, the surangular portion of the mandibular glenoid is deep and expanded both rostrocaudally and mediolaterally, extending above the lateral side of the surangular. A low, round ridge running obliquely from the lateral lip toward the medial base of the retroarticular process subdivides the glenoid. The retroarticular process is elongate but slender: it is compressed medio-laterally and its ventral border is particularly thin indeed. The tip of the retroarticular process is turned laterally. In front of the glenoid, the high and thin rostral plate of the surangular forms the caudolateral wall of the large adductor fossa. The insertion area for *M. pterygoideus* forms a particularly long and deep rectangular facet under the glenoid on the medial side of the surangular. It is separated from the medioventral elongated facet for the angular by a prominent horizontal crest. According to Horner (1992), this shelf contacted the splenial.

Teeth.—As is usual in hadrosaurids, maxillary teeth are miniaturised and of simple morphology. They are narrow, diamond-shaped, perfectly straight, and symmetrical. The enamel forms a strong and perfectly straight median ridge on the lateral side of the crown. Both borders of the crown are slightly denticulate.

The dentary teeth are also diamond-shaped and dorsoventrally elongated. However, they look proportionally wider than the maxillary teeth, with a "height/width" ratio of about 3.5 for the teeth located in the middle of the dental battery. The lateral denticulations are better developed than on the maxillary teeth; the median carina is, on the other hand, less developed. The median carina is perfectly straight on the distal and central dentary teeth, but it is slightly sinuous on the mesial ones. Incipient secondary ridges are sporadically developed on the dentary teeth, both mesial and distal to the median carina). The presence of secondary ridges on dentary teeth is usually regarded as a plesiomorphic character of Hadrosauroidea. However, careful examination of species reveals that these ridges exist in several other Hadrosauridae, such as *Aralosaurus tuberiferus*, *Saurolophus angustirostris* (personal observations), *Parasaurolophus* sp. (see Horner 1990: fig. 13.4, d), *Gryposaurus latidens* (see Horner 1992: pl. 42, e), or *Pararhabdodon isonensis* (see Casanovas et al. 1999). The root of the dentary teeth is always high and mesio-distally compressed. Although this character is highly variable, even within the same dental battery (see AEHM 1/12), the angle between the crown and the root of dentary teeth is always higher than 145°.

Axial skeleton

This descriptive section devoted to the axial skeleton will be short, because of the nature of the studied material. As most of the material belongs to juveniles, centra and neural arches are found disarticulated in the bonebed. Moreover, most of the neural spines and processes are completely broken off

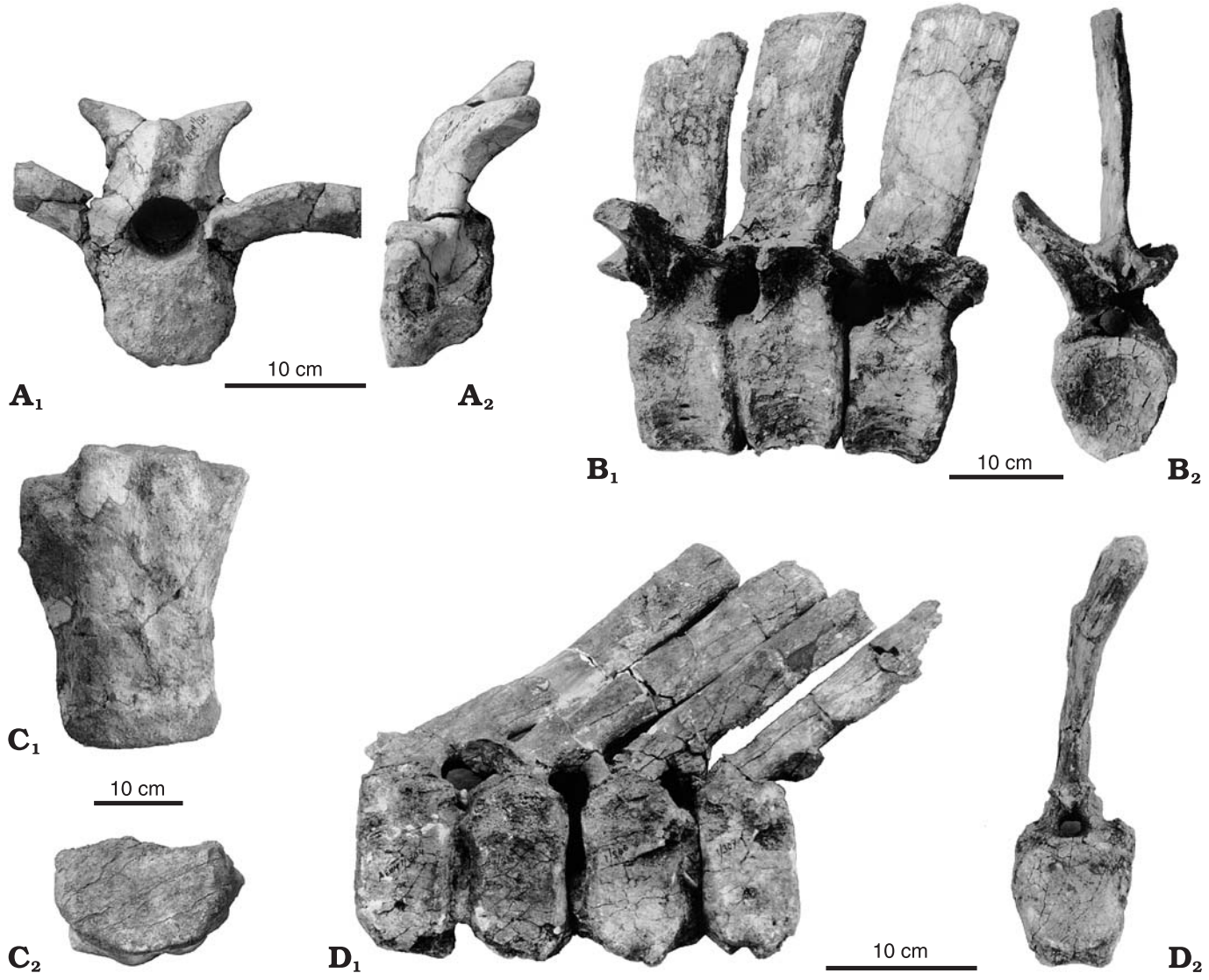

Fig. 12. *Amurosaurus riabinini*. **A**. Cranial cervical vertebra (AEHM 1/275) in cranial (A_1) and left lateral (A_2) views. **B**. Dorsal vertebrae (AEHM 1/297–299) in left lateral (B_1) and caudal (B_2) views. **C**. Partial sacrum (AEHM 1/296) in ventral (C_1) and cranial (C_2) views. **D**. Caudal vertebrae (AEHM 1/304–307) in left lateral (D_1) and caudal (D_2) views.

during transportation. Ribs are fragmentary and of typical hadrosaurid morphology, devoid of diagnostic character. Herein we simply describe some well-preserved or articulated material belonging to adult specimens.

Cervical vertebrae (Fig. 12A).—The centrum of the cranialmost cervical vertebrae is strongly opisthocoelous, with a globular cranial articular surface and a cup-shaped caudal surface. These centra are particularly wide, with the following proportions: width > height = length. The ventral side of the centrum bears a longitudinal keel that may be bordered dorsally by a pair of small nutritive foramina. Between the articular surfaces, the lateral sides of the centrum are slightly depressed. The parapophyses are not prominent and set at midheight on the lateral sides of the centrum, close to the cranial border. The neural arch surrounds a large neural canal. The lateral transverse processes are long, stout and strongly curved backwardly. Their mediodorsal side bears large elliptical prezygapophyses whose flat surface faces upwardly, inwardly, and slightly forwardly. The tip of each transverse process bears a small diapophysis. The postzygapophyesal processes are long and curved; they diverge backwardly and outwardly. Distally, their ventral side bears a large elliptical postzygapophysis whose flat surface faces downwardly, outwardly, and backwardly. Although the studied material is fragmentary, the following changes can be observed on the more caudal cervical vertebrae:

- The postzygapophyseal processes are fused.
- The neural spine forms a hook-like blade.
- The transverse processes become larger, stouter, and more curved downwardly and backwardly.
- The parapophyses migrate dorsally from the middle of the lateral sides of the centrum to the base of the transverse processes.

Dorsal vertebrae (Fig. 12B).—Six articulated vertebrae (AEHM 1/297–302) belong to the central part of the dorsal series. Their centra are unusually opisthocoelous: the cranial articular side is slightly convex, whereas the caudal side is strongly concave. Both articular surfaces of the centrum are typically heart-shaped with the following proportion: height > width > length. A strong ridge runs along the ventral side of the centrum, joining both articular surfaces. Above the ridge, the lateral sides of the centrum are strongly contracted and pierced by several irregularly distributed nutritive foramina. The neural arch is robust. The prezygapophyses are wide, with a cranio-caudal long axis. They are slightly concave and face inwardly, upwardly, and a little forwardly. A thin median vertical ridge from the base of the neural spine separates the prezygapophyses from each other. The postzygapophyses are also wide and slightly concave, with a cranio-caudal long axis; they face downwardly, outwardly, and slightly backwardly. A small indentation separates them at the base of the neural spine. The diapophyses are elongate, strong, and inclined backwardly and upwardly. Their cranial border joins the apex of the prezygapophyses, while their caudal border joins the apex of the postzygapophyses. The ventral side of the diapophyses bears a strong curved ridge that extends toward the caudoventral corner of the neural arch. This ridge forms the ventrolateral margin of extremely excavated fossae on the caudal side of the neural arch below the postzygapophyses. These fossae are separated from each other by a median ridge from the base of the postzygapophyses to the roof of the neural canal. The parapophyses form slight kidney-shaped processes between the diapophyses and prezygapophyses. The neural canal is wider than high. The neural spines are subrectangular in lateral view, robust and about three times as high as long. Their apex is slightly enlarged, both cranio-caudally and laterally, and rough, indicating the possible presence of a cartilage cap in life. The orientation of the neural spine is variable, depending on the position within the dorsal series: in the six articulated vertebrae, the spine is slightly inclined forwardly, whereas it may be inclined backwardly in other specimens.

Sacrum (Fig. 12C).—An eroded partial sacrum preserved in the material from Blagoveschensk is formed by two fused centra whose dorsal portion is completely destroyed. The articular surfaces are elliptical in outline, wider than high, and slightly concave. The sacral fragment is wider caudally than cranially. The lateral sides are so badly preserved that they cannot be adequately described. A broad and shallow sulcus is developed along the ventral side of the sacrum. Several authors have previously debated the phylogenetic significance of this character. Gilmore (1933) first observed that such a groove characterizes the sacrum of Hadrosaurinae, whereas that of Lambeosaurinae bears a longitudinal ridge. Weishampel and Horner (1990) and Horner (1990) subsequently followed this opinion. Weishampel et al. (1993), on the other hand, identified the ventral groove as a synapomorphy for Lambeosaurinae. Godefroit et al. (1998) and Norman (1998) showed that this feature is in fact not consistent in non-hadrosaurid Hadrosauriformes. Godefroit et al. (2001) showed that it clearly requires revision in Hadrosauridae as well, because the sacrum of *Charonosaurus jiayinensis* bears both sulcus and ridge. In the current state of our knowledge it is therefore impossible to state whether the grooved fragmentary sacrum described herein really belongs to *Amurosaurus riabinini*, or to some hadrosaurine living in the same area. Indeed, hadrosaurine bones, although rare when compared to the lambeosaurine ones, have also been discovered at Blagoveschensk (Bolotsky and Godefroit 2004).

Caudal vertebrae (Fig. 12D).—Seven vertebrae belonging to the proximal portion of the tail have been discovered in articulation. The centra are typically amphiplatyan, with subrectangular articular surfaces. Between the articular surfaces, the lateral sides of the centra are slightly depressed and pierced by irregularly distributed nutritive foramina. The articular facets for the sacral ribs are ovoid, concave, and rough; they extend on the lateral side of both the centrum and neural arch. The ventral side of the centrum is slightly concave. The four lateroventral corners are truncated by large and concave haemapophyseal facets with slightly everted edges. The neural arch of the caudal vertebrae is less robust than that of the dorsal vertebrae and the size of the neural canal is smaller. The prezygapophyses are inclined inwardly, whereas the postzygapophyses are similarly inclined outwardly. The neural spine is long, slender, and steeply inclined backwardly and slightly curved dorsally. The tip of the neural spine is slightly expanded transversely and rough, but it is not particularly club-shaped as in *Barsboldia sicinskii* Maryańska and Osmólska, 1981b. Traces of ossified ligaments lie along the lateral sides of the neural spine of many specimens. Toward the distal end of the tail, the following trends in the morphology of the caudal vertebrae may be observed:

- The centrum becomes proportionally longer, wider, and less elevated.
- The articular surfaces become hexagonal in outline.
- The articular facets for the caudal ribs progressively disappear.
- The haemapophyseal facets lessen in size.
- The relative size of the neural canal, the neural arch, and the zygapophyses decreases.
- The length of the neural spine decreases, while it progressively becomes more steeply inclined backwardly and more curved.

Pectoral girdle and forelimb

Scapula (Fig. 13C).—As noted by Brett-Surman (1989), the hadrosaurid scapula lies parallel to the vertebral column in natural articulation. Its "upper" margin is therefore described herein as dorsal, and its "lower" margin as ventral. In *Amurosaurus riabinini*, the proximal head of the scapula appears

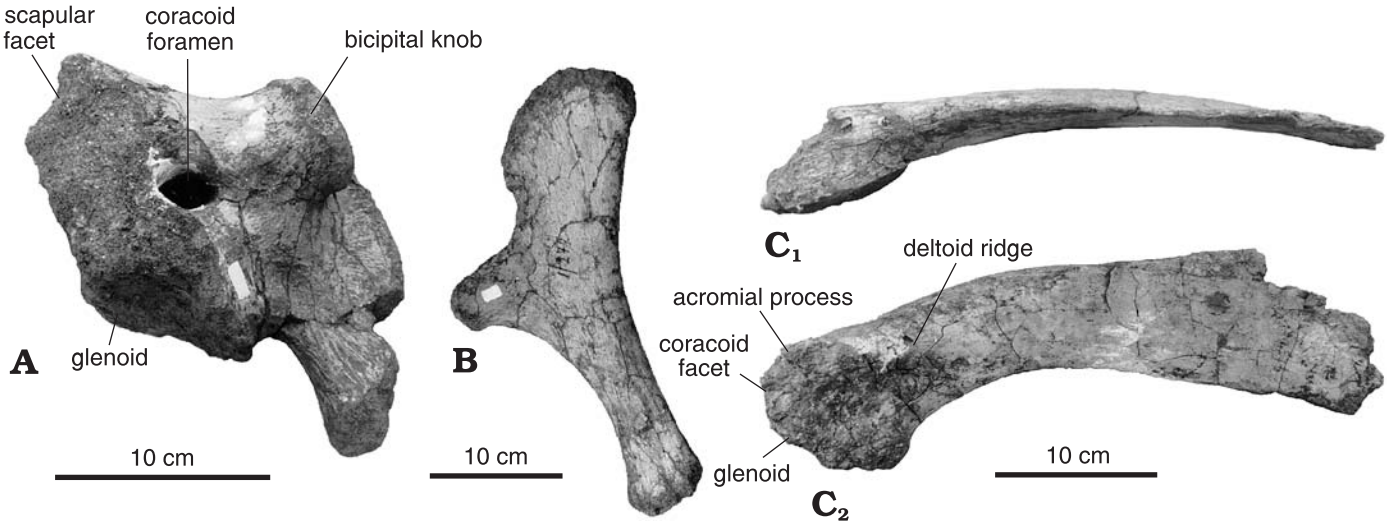

Fig. 13. *Amurosaurus riabinini*. **A**. Right coracoid (AEHM 1/271) in cranial view. **B**. Right sternum (AEHM 1/272) in caudal view. **C**. Left scapula (AEHM 1/273) in ventral (C_1) and lateral (C_2) views.

less robust than in *Charonosaurus jiayinensis*. The coracoid suture is large and cup-shaped. Above this area, the lateral side of the proximal head forms the acromial process that extends caudoventrally in the form of a short round deltoid ridge. Above the acromial process, longitudinal striations indicate the insertion area for *M. trapezius*. The deltoid fossa is not particularly enlarged. Ventral to the coracoid suture, a long crescentic depression facing slightly laterally represents the dorsal part of the glenoid. The cranioventral process of the scapula, which formed the caudodorsal margin of the glenoid, is only moderately developed. The scapular blade is long and dorsoventrally narrow, with a "length/width" ratio (*sensu* Brett-Surman 1989) > 4.5, and also deflected ventrally. According to Godefroit et al. (2001), the elongation and ventral curvature of the scapular blade may be related to a general increasing of the power of the forelimb, as it lengthens the in-lever arms of *M. teres major*, which inserted along the caudoventral side of the scapular blade. The scapular blade of *Amurosaurus riabinini* is also distinctly curved inwardly. Its lateral side is slightly convex dorsoventrally, whereas its medial side is perfectly flat.

Coracoid (Fig. 13A).—The most striking character of the coracoid of *Amurosaurus riabinini* is its massiveness. Extremely thick caudally, it progressively becomes thinner cranially. It forms a prominent cranioventral hooklike process. The cranial border of the coracoid is deeply grooved and pitted, indicating the presence of a cartilaginous cap. Around this border, both medial and lateral sides of the coracoid bear numerous, strong, and radiating ridges that probably indicate an extensive attachment site for a powerful *M. coracobrachialis*. At the level of its craniodorsal angle, the lateral side of the coracoid bears an extremely prominent knob, whose dorsolaterally-facing surface served as attachment site for a strong *M. biceps.* Under the bicipital knob, the coracoid bears a well-marked depressed area for insertion of *M. triceps coracoscapularis*. The coracoid foramen is large and elliptical; it is always completely surrounded by the coracoid. Both the scapular articular surface and the glenoid are well developed on the caudal side of the coracoid, together forming an angle of about 120°. The articular surface for the scapula is slightly concave and rough, with numerous knobs and depressions. The glenoid is cup-shaped, facing caudoventrally and slightly laterally.

Sternum (Fig. 13B).—The sternum of *Amurosaurus riabinini* is also a massive element. It is typically hatchet-shaped and dorsoventrally compressed, as in other hadrosaurids. Its proximal plate is enlarged both in length and width. It is thinner laterally then medially. Although incompletely preserved, the thin lateral border of the proximal plate appears distinctly concave. The distal "handle" of the sternal is relatively short, but massive and slightly curved dorsally; the distal end of the "handle" is slightly enlarged. Both the proximal and distal borders of the sternal are rough, indicating the presence of cartilagineous caps. The ventral side of the sternal is slightly convex mediolaterally, whereas its dorsal side is slightly concave.

Humerus (Fig. 14A).—The humerus of *Amurosaurus riabinini* is typically lambeosaurine in shape, with a long and wide deltopectoral crest. It is interesting to observe that this crest is apparently better developed in larger adult specimens than in juveniles, as previously noted by Brett-Surman (1989); this crest is slightly convex in juveniles, whereas it is straighter in larger specimens. The deltopectoral crest is slightly turned medially. The globular proximal articular head forms a round buttress on the caudal side of the humerus. The inner tuberosity is poorly developed, whereas the outer tuberosity is larger. On the caudal side of the humerus, a smooth round crest descends from the proximal articular

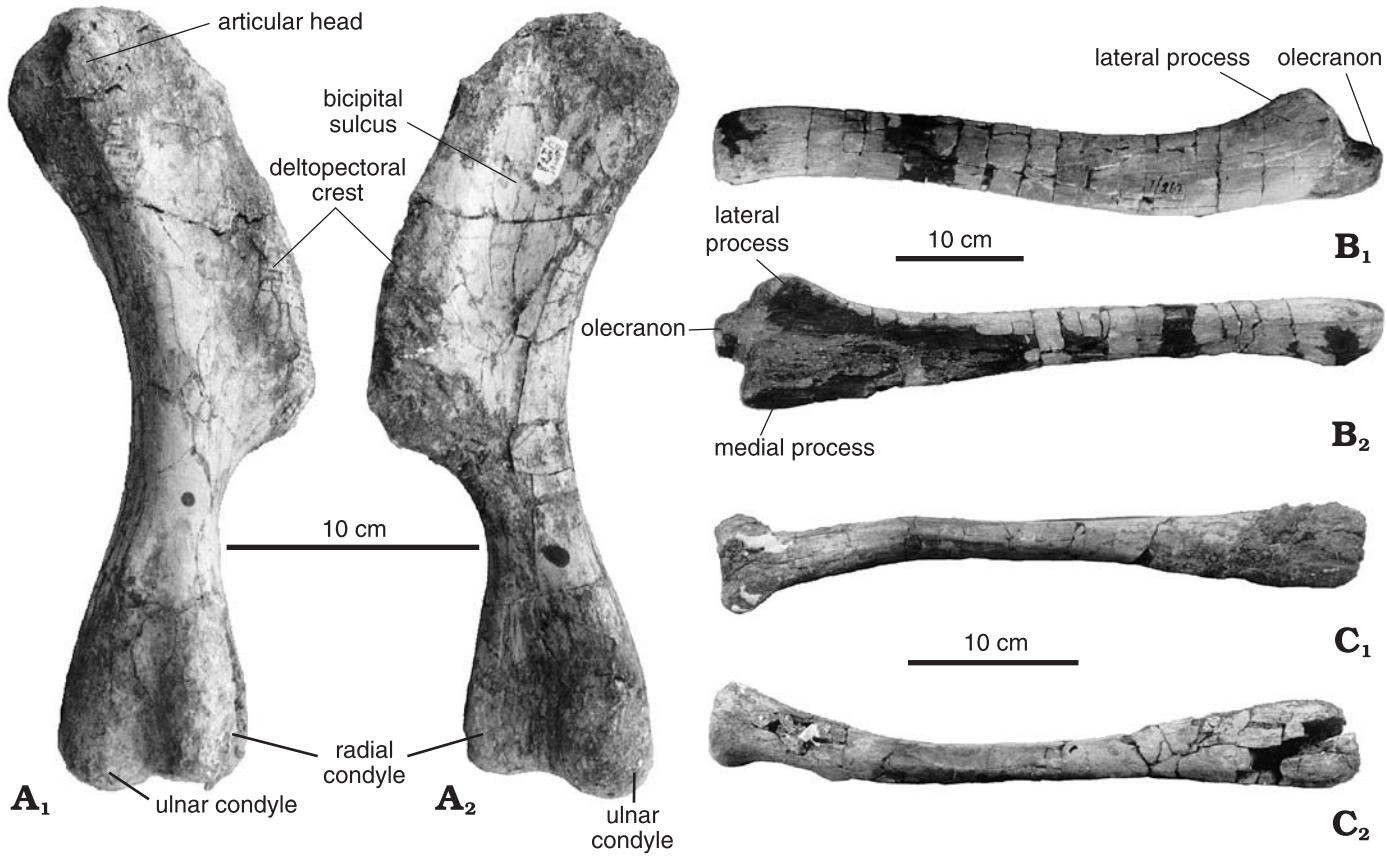

Fig. 14. *Amurosaurus riabinini*. **A**. Right humerus (AEHM 1/278) in caudal (A_1) and cranial (A_2) views. **B**. Left ulna (AEHM 1/267) in lateral (B_1) and cranial (B_2) views. **C**. Left radius (AEHM 1/268) in caudal (C_1) and medial (C_2) views.

head, but is never as well developed as in *Charonosaurus jiayinensis* (see Godefroit et al. 2000). On the cranial side of the humerus, the bicipital groove is also less well-marked than in *Charonosaurus jiayinensis*. Lateral to the humeral head, a large depressed area marks the insertion of a strong *M. triceps humeralis posticus*. Medial to the humeral head, a less depressed area indicates the insertion of *M. scapulo–humeralis*. The distal portion of the humerus is slender and slightly twisted outwardly. The ulnar condyle is slightly better developed than the radial condyle, and the intercondylar groove is wider on the cranial side than on the caudal side of the humerus.

Ulna (Fig. 14B).—The ulna of *Amurosaurus riabinini* is robust. In cranial view, this bone displays a characteristic sigmoidal curvature: its proximal part is convex medially, whereas its distal part is convex laterally. It is also distinctly sigmoidal in medial or lateral view: the proximal end is convex caudally, whereas the distal part is convex cranially. The olecranon process is never prominent but, as previously noted by Brett-Surman (1989), it is better developed in juveniles than in larger specimens. The olecranon notch is well developed, especially in larger specimens. The medial proximal process is partcularly high and robust, whereas the lateral process is distinctly lower and thinner. Between both processes, the articular facet for the proximal part of the radius is particularly enlarged and triangular in shape; longitudinal striations indicate strong ligamentous attachment with the radius. Under this area, the body of the ulna is particularly high craniocaudally. The ulna progressively tapers distally. Its distal end is round, laterally compressed and triangular in cross-section. The large triangular articular surface for the distal end of the radius faces craniomedially; it also bears strong longitudinal striations.

Radius (Fig. 14C).—In contrast to the ulna, the radius of *Amurosaurus riabinini* is gracile. However, it is also clearly sigmoidal in shape, both in cranial and in lateral views. The proximal end of the radius is well-expanded, resembling the top of a Doric column in cranial view, as previously described by Brett-Surman (1989); its cranial side is slightly convex, whereas its caudal side is flat where it articulated with the proximal part of the ulna. The distal end of the radius is round and triangular in cross-section; it is also slightly expanded mainly mediolaterally. Its flat caudolateral side is applied to the distal part of the ulna.

Metacarpals.—The metacarpals of *Amurosaurus riabinini* are elongated pencil-shaped bones with smooth featureless articular ends. Metacarpal II is the most slender element of

the series. Both its articular ends are only slightly expanded and round. The lateral side of metacarpal II is regularly convex, whereas its medial side is slightly concave along its entire length and bears longitudinal striations for ligamentous attachment with metacarpal III. Metacarpal III is the stoutest of the series. It is triangular in cross-section along its entire length. Its proximal articular head is slightly more expanded and round than its distal end. Both its dorsomedial and dorsolateral sides bear longitudinal striations for strong ligamentous attachment with adjacent metacarpals. Unlike metacarpals II and III, which are perfectly straight, metacarpal IV is curved laterally. Its proximal head is turned so that its flat medial side covers the dorsolateral side of metacarpal III. Its shaft is subrectangular in cross-section. Its distal end is flat mediolaterally, slightly expanded palmodorsally, and round.

Manual phalanges.—Some isolated phalanges of the hand are preserved in the Blagoveschensk collection. All are slender and flat hourglass-shaped elements, ovoid in cross-section. Their slightly expanded articular surfaces are smoothly convex and featureless. The proportions of these bones are variable, reflecting the position of the phalanx within the hand. However, the simple morphology of these elements makes it difficult to recognise the exact position of each element.

Pelvic girdle and hindlimb

Pubis (Fig. 15A).—The prepubis is composed of a cranial blade and a neck connecting it to the middle part of the pubis. Because they are thin, the margins of the prepubic blade are not completely preserved. However, the blade appears well-expanded both dorsally and ventrally, with a round cranial border. In cranial view, the prepubic blade is slightly concave laterally, with the ventral border set more laterally than the dorsal border. The prepubic neck is relatively short and robust. Its dorsal border is round, whereas its ventral border is particularly sharp. The prepubic process of *Amurosaurus riabinini* appears to be intermediate in shape between that of *Corythosaurus casuarius* ("Type 4" of Brett-Surman 1989) and the robust process of *Parasaurolophus cyrtocristatus* ("Type 5" of Brett-Surman 1989). The middle part of the pubis is thickened and formed by two robust peduncles for intimate contact with the adjacent bones of the pelvic girdle. The iliac peduncle is stout and triangular in cross-section, with a round and rough dorsal border. Its lateral side bears a strong and rough crest that forms the cranial limit of a laterally-facing area, the pubic part of the acetabulum. Medially, the iliac peduncle bears a well-marked elliptical facet for contact with one of the cranialmost sacral ribs. The ischial peduncle is particularly elongated and expanded caudally where it contacts the pubic bar. Its lateral side bears a strong horizontal ridge that forms the ventral cranioventral limit of the acetabulum. The caudoventrally-projecting pubic shaft is incompletely preserved. It is stout and triangular in cross-section. The ischial peduncle and the pubic shaft enclose a craniocaudally-elongate obturator foramen.

Ischium (Fig. 15C).—Of the many ischia that have been discovered at Blagoveschensk, all unfortunately are badly preserved. The cranial part of the ischium is elongate and flat mediolaterally; as usually described in ornithopods, it is triradiate, composed of an iliac ramus, a pubic ramus and an obturator process. The iliac ramus is elongate, but its cranial end is not particularly thickened. It projects craniodorsally, forming an angle of about 145° with the ischial shaft; this angle is very open as usually observed in lambeosaurines (see Brett-Surman 1989: pl. 8). The pubic ramus of the ischium is short and the ischial part of the acetabulum is not particularly deep: this character may be correlated to the important elongation of the ischial peduncle of the pubis that consequently formed the greatest part of the ventral margin of the acetabulum. On the caudoventral part of the proximal blade of the ischium, the obturator process is small, as observed for example in *Corythosaurus casuarius* (see Brett-Surman 1989: pl. 6); it is much more developed in *Parasaurolophus cyrtocristatus*, where it is as large as the pubic ramus. Between the pubic ramus and obturator process, the obturator foramen is deep and completely open. The ischial shaft is long, slender, and perfectly straight. It has a kidney-like outline, with a regularly convex lateral side and a slightly concave medial side; its diameter does not change along its entire length. Farther caudally, it gradually thickens; unfortunately, the distal end of the ischium is never preserved in the material discovered to date, so that it is not possible to assess whether it really ends into a foot-like structure, as is usually observed in lambeosaurines. Strong longitudinal striations run along the medial concavity of the ischial shaft, indicating tight ligamentous attachment between paired ischia.

Ilium (Fig. 15B).—The ilium of *Amurosaurus riabinini* closely resembles that of Lambeosaurinae referred to the *Corythosaurus* lineage by Brett-Surman (1989: pl. 4D, *Lambeosaurus lambei*). The preacetabular process forms a tapering projection from the iliac blade; it is robust and deflected ventrally. Although always incomplete, this process does not look as long as that in *Charonosaurus jiayinensis*. Its ventral border is round, whereas its dorsal border is thinner and inclined medially. The caudal portion of its medial side bears a strong longitudinal ridge; it starts at mid-height between the dorsal and ventral borders of the preacetabular process and extends obliquely toward the iliac blade to fuse with the dorsal border of the ilium at the level of the ischial peduncle. Although its ventral part is damaged in all specimens discovered to date, the iliac blade appears to be relatively high, as in *Lambeosaurus lambei*, but distinctly lower than in *Parasaurolophus cyrtocristatus* or *Charonosaurus jiayinensis*. At the level of the ischial peduncle, the lateral side of the iliac blade forms a prominent antitrochanter. The dorsolateral side of this bone served as attachment site for a

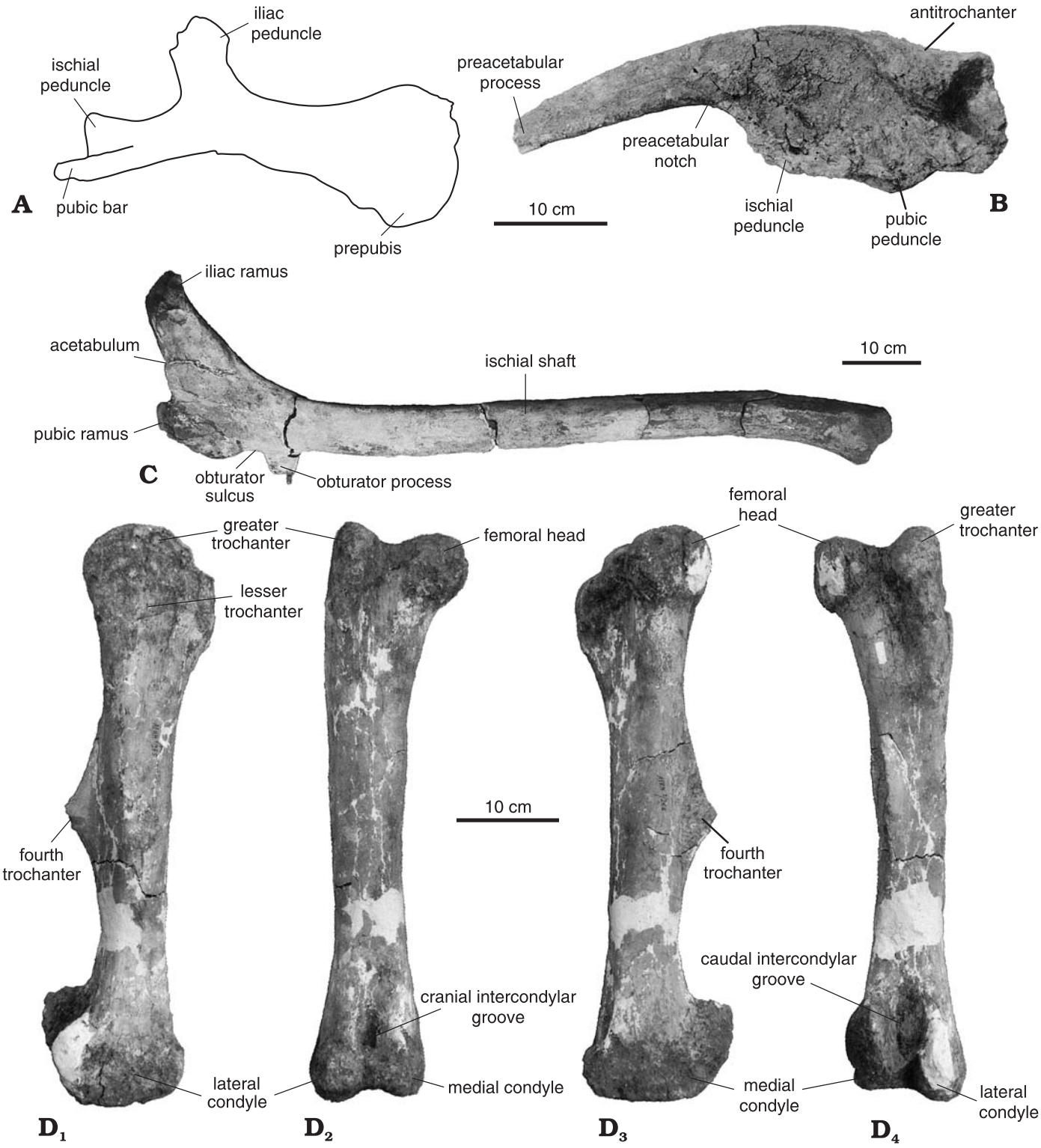

Fig. 15. *Amurosaurus riabinini*. **A**. Diagrammatical drawing of the left pubis (AEHM 1/263) in medial view. **B**. Left ilium (AEHM 1/264) in lateral view. **C**. Left ischium (AEHM 1/269) in lateral view. **D**. Right femur (AEHM 1/265) in lateral (D_1), cranial (D_2), medial (D_3), and caudal (D_4) views.

powerful *M. ilio-femoralis*. However, this process is not as well developed as in *Parasaurolophus cyrtocristatus* or *Charonosaurus jiayinensis*. The preacetabular notch is very open. The postacetabular process is always broken off.

Femur (Fig. 15D).—The femur of *Amurosaurus riabinini* is robust. The femoral head is well developed and globular in shape. It is set at an angle to the shaft on a stout and short neck and is connected by a low ridge to the greater trochanter

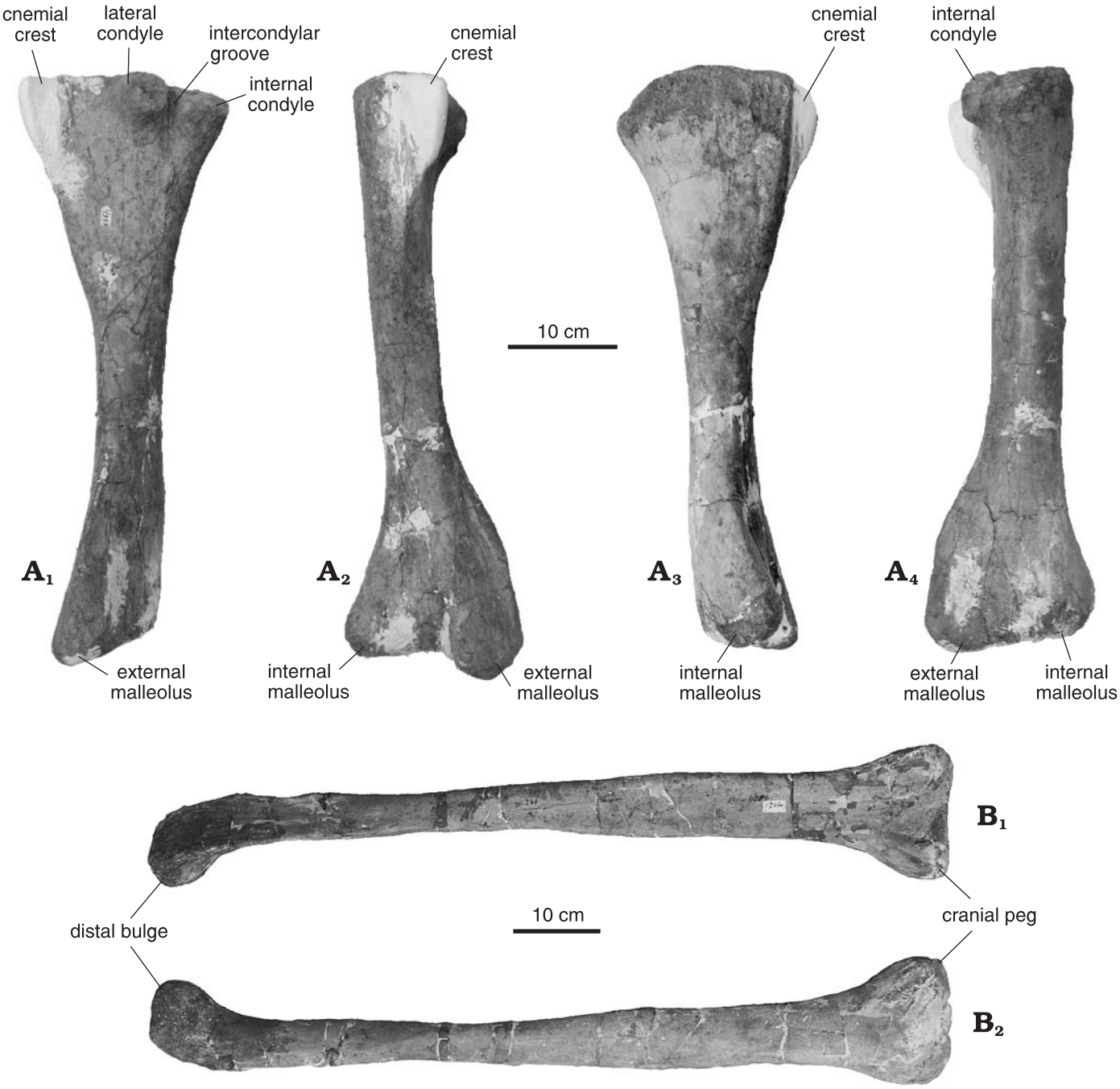

Fig. 16. *Amurosaurus riabinini*. **A**. Left tibia (AEHM 1/969) in lateral (A_1), cranial (A_2), medial (A_3) and caudal (A_4) views. **B**. Left fibula (AEHM 1/266) in medial (B_1) and lateral (B_2) views.

on the proximomedial angle of the bone. The greater trochanter is more extended craniocaudally than the femoral head, but its apex lies a little lower than that of the latter. The lateral side of the greater trochanter is depressed by a large triangular insertion area for *M. ilio-trochantericus* 1. The lesser trochanter is well developed on the craniolateral side of the proximal portion of the femur, especially in juvenile specimens. It is separated from the greater trochanter by a shallow cleft. It extends as a short round ridge along the craniolateral angle of the proximal part of the femoral shaft. *M. ilio-femoralis* inserted along a well developed triangular area on the lateral side of the lesser trochanter. The femoral shaft is long, very robust, and quadrangular in cross-section. The fourth trochanter forms a prominent, thin, and triangular process at midshaft along the caudomedial side of the femur. Its entire medial side is deeply excavated by a large insertion area for a powerful *M. caudi-femoralis longus*. A rectangular scar along the dorsolateral side of the fourth trochanter may be interpretated as the insertion area for *M. caudi-femoralis brevis*. In front of the fourth trochanter and slightly more dor-

sally, a depressed and extended facet is interpretated as the insertion area for *M. pubo-ischio-femoralis internus* 1 (Norman 1986). The distal condyles are expanded craniocaudally, with regularly convex articular surfaces. The medial condyle is higher and extends farther caudally than the lateral condyle. The caudal extension of the distal condyles is greater than their cranial extension. Cranially, the condyles are fused together to form an intercondylar "tunnel" that surrounded and protected the distal tendon of *M. ilio-tibialis* above the knee. Caudally, the distal condyles are separated from each other by a wide and deep intercondylar groove.

Tibia (Fig. 16A).—The proximal head of the tibia is enlarged craniocaudally, especially in larger specimens. Its cranioproximal corner forms a large wing-like cnemial crest, stongly deflected laterally. Along the cranial part of the cnemial crest, a large depressed facet marks the insertion area for the strong distal ligament of *M. ilio-tibialis*. The medial side of the proximal head of the tibia is regularly convex. Its caudal corner forms a large internal condyle separated by a deep, but narrow groove from the smaller lateral condyle. The tibial shaft is long, straight, and ovoid in cross-section. Because of the distal extension of the cnemial crest, the long axis of its proximal portion is oriented craniocaudally. This axis progressively becomes oriented mediolaterally toward its distal end. The tibial shaft bears a prominent lateral ridge that extends distally to form the lateral corner of the external malleolus. The distal end of the tibia is enlarged medio-laterally. The external malleolus is prominent distally; its articular surface is turned toward the caudomedial side of the tibia. The internal malleolus is, on the other hand, more prominent medially, with an articular surface turned toward the craniolateral side of the tibia.

Fibula (Fig. 16B).—The fibula of *Amurosaurus riabinini* is straight and slender. Its proximal end is widened craniocaudally, forming a cranial peg. The diameter of the fibula progressively decreases distally. Its lateral side is smoothly convex along its entire length. The medial side, on the other hand, is occupied by two high concave triangular surfaces. The upper surface points distally and occupies the proximal two-thirds of the fibular shaft; it bears elongated striations for ligamentous contact with the tibia. The second triangular surface points proximally and occupies the distal third of the medial side of the fibula; its very striated surface faces caudomedially to fit against the external malleolus of the tibia. The distal end of the fibula forms an enlarged craniolateral bulge: its articular surface is ball-shaped, perfectly round, and rough to fit into the calcaneus. However, this bulge is distinctly less expanded than in *Parasaurolophus cyrtocristatus* or *Charonosaurus jiayinensis*.

Astragalus (Fig. 17A).—The astragalus of *Amurosaurus riabinini* is particularly wide mediolaterally, but low. In dorsal view, it is round, whereas that of *Charonosaurus jiayinensis* is more rectangular. The articular surface for the internal malleolus of the tibia is wide, occupying the medial two-thirds of the dorsal side; this surface is slightly concave and faces craniomedially. The articular surface for the external malleolus of the tibia forms the lateral third of the dorsal surface of the astragalus; it is concave and faces laterally. A low, oblique, and round ridge separates both articular surfaces that join together the caudal and cranial ascending processes. The caudal process, which accommodated against the caudal side of the tibia, is elongated, but low; it is set medially, but unlike in *Charonosaurius jiayinensis*, it does not form the craniomedial angle of the astragalus. The cranial ascending process is slightly higher and set on the craniolateral corner of the astragalus. In cranial view, it is sub-triangular and only slightly skewed laterally. Its is thus intermediate in shape between the equilateral cranial ascending process of *Charonosaurus jiayinensis* and *Parasaurolophus cyrtocristatus*, and the laterally skewed process of other North-American hadrosaurids (Brett-Surman 1989). Like in *Charonosaurus jiayinensis* and *Parasaurolophus cyrtocristatus*, the cranial side of the cranial ascending process is strongly depressed. The ventral side of the astragalus is regularly convex craniocaudally and concave mediolaterally.

Calcaneus.—The calcaneus of *Amurosaurus riabinini* is stout and subtrapezoidal, much more elongated craniocaudally than mediolaterally. Its ventral side is regularly round. Unfortunately, the dorsal surface of the only preserved specimen is destroyed, so that the ascending process cannot be accurately described. An oblique transverse ridge separates the two articular surfaces from each other. The cranial articular facet for the fibula is larger craniocaudally, but narrower mediolaterally than the caudal articular surface for the tibia. The dorsal surface of the fibular facet is only slightly concave, but rough; the tibial facet is much deeper. The lateral side of the calcaneus is depressed under the ascending process.

Metatarsals (Fig. 17B–D).—The metatarsals of *Amurosaurus riabinini* are robust, as usually observed in hadrosaurids. **Metatarsal II** is compressed mediolaterally. Its medial surface is smoothly convex, whereas its lateral side is flat and bears longitudinal striations marking strong attachment to metatarsal III. The proximal end of metatarsal II is not expanded plantodorsally, being only a little wider than the distal end. The proximal articular surface is round and rough. Beneath the middle of the shaft, the dorsolateral border of metatarsal II forms a prominent liplike projection that reinforced attachment with metatarsal III. Beneath the lip, the shaft of metatarsal II diverges medially from metatarsal III. The distal articular end is regularly convex plantodorsally, but does not display any trace of an intercondylar groove. **Metatarsal III** is the stoutest of the series. Its proximal articular end is subtriangular, slightly convex, and more developed plantodorsally than mediolaterally. Its proximomedial side forms a large concave surface for reception of metatarsal II. The shaft of metatarsal III is contracted both plantodorsally and mediolaterally. The distal end of metatarsal III is slightly expanded to form a large saddle-shaped articular surface. The plantodorsal intercondylar groove is well devel-

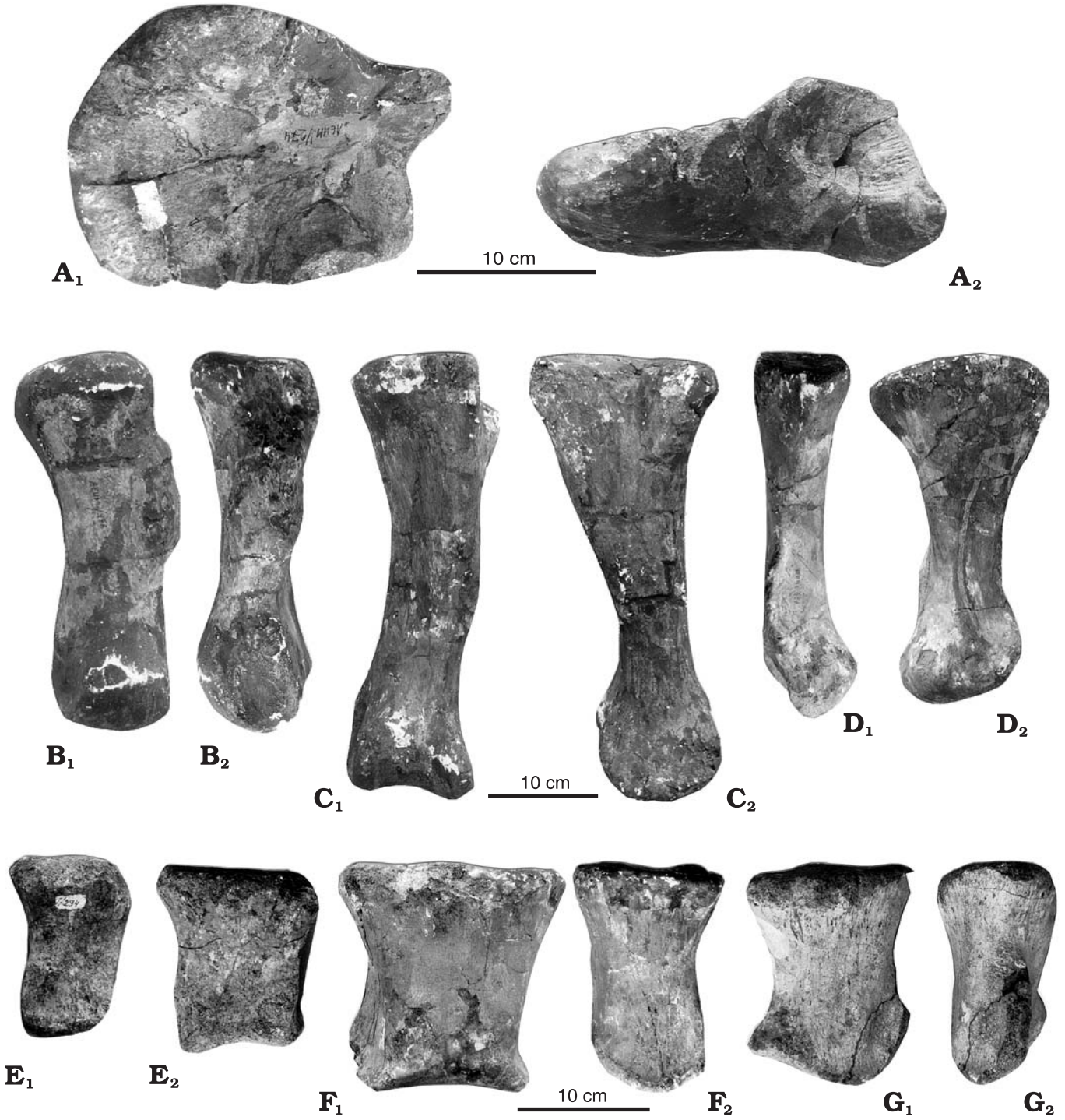

Fig. 17. *Amurosaurus riabinini*. **A**. Left astragalus (AEHM 1/274) in dorsal (A_1) and cranial (A_2) views. **B**. Right metatarsal IV (AEHM 1/286) in dorsal (B_1) and medial (B_2) views. **C**. Right metatarsal III (AEHM 1/285) in dorsal (C_1) and medial (C_2) views. **D**. Left metatarsal II (AEHM 1/284; mirror image) in dorsal (D_1) and medial (D_2) views. **E**. Right 4th proximal phalanx (AEHM 1/294) in lateral (E_1) and dorsal (E_2) views. **F**. Right 3rd proximal phalanx (AEHM 1/283) in dorsal (F_1) and medial (F_2) views. **G**. Right 2nd proximal phalanx (AEHM 1/292) in dorsal (G_1) ans medial (G_2) views.

oped. The medial side of the distal articular end forms a cup-like depression. **Metatarsal IV** is more slender than metatarsal III. Its proximal articular surface is semicirular and more expanded plantodorsally than mediolaterally. It is cup-shaped for reception of the fourth distal tarsal. Beneath the proximal head, the medial side of metatarsal IV forms a wide triangular depressed area, bearing strong longitudinal striations and extending distally toward the level of the middle of the shaft. Distal to this area, its dorsomedial side bears a strong knob that was applied to the lateral side of metatarsal III. A plantomedial lip also overlapped metatarsal III. The distal part of metatarsal IV curves laterally away from meta-

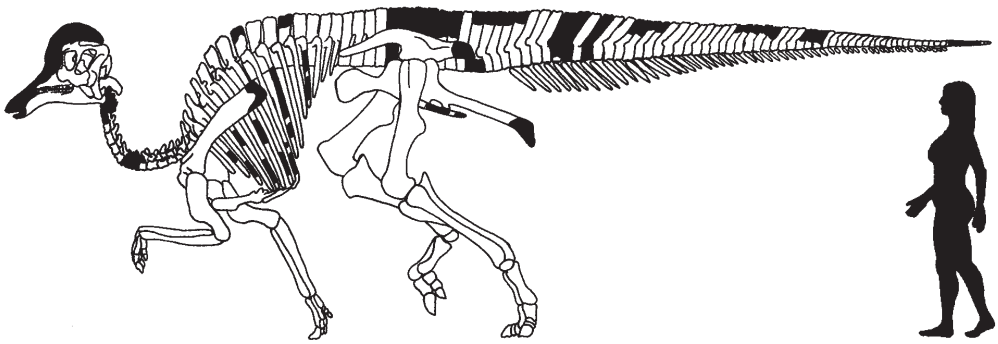

Fig. 18. Skeletal reconstruction of *Amurosaurus riabinini* Bolotsky and Kurzanov, 1991. Black elements are not preserved in the available material.

tarsal III. The distal articular head is expanded plantodorsally to form a saddle-like oblique articular condyle, bearing a shallow intercondylar groove.

Pedal phalanges (Fig. 17E–G).—The proximal phalanges are massive block-like bones with a broad and concave proximal articular surface and a less expanded, but saddle-like distal trochlea. A flat scarred area for insertion of the flexor tendons is present on the proximoplantar part of these phalanges. The proximal phalanx of digit II is more slender than the others and asymmetrical: its lateral side is more convex, higher, and more vertical than its medial side. That for digit III is the stoutest of the series, with a more concave proximal articular surface and a better developed distal trochlea. It is perfectly symmetrical in dorsal view; both its medial and lateral sides are steeply inclined, so that its plantar surface is wider than its dorsal surface. The proximal phalanx for digit IV is proportionally the shortest and the thickest of the series. Its medial side is elevated and slightly concave; its lateral side is a little less high and vertical. **The intermediate phalanges** are short, but wide elements with a concave proximal articular surface and convex distal surface. Between both articular surfaces, the dorsal and plantar sides are depressed and rough. **The ungual phalanges** are proportionally wide and hoof-like. They are arched and flat plantodorsally toward their tip. The plantar side bears well-marked claw-grooves converging toward the tip of the bone. The rounded distal margin is always rough.

Fig. 18 is a composite reconstruction of the skeleton of *Amurosaurus riabinini*, based on the different elements described above.

Comparisons with other Lambeosaurinae from the Amur region

In addition to *Amurosaurus riabinini*, two other lambeosaurine taxa have been described from the Maastrichtian of the Amur region: *Charonosaurus jiayinensis* Godefroit, Zan, and Jin, 2000 from the Jiayin locality along the Chinese banks of Amur River and *Olorotitan arharensis* Godefroit, Bolotsky, and Alifanov, 2003 from the Kundur locality. *Olorotitan* was also discovered in the Udurchukan Formation (Godefroit et al. 2003). *Charonosaurus* was discovered in the Yuliangze Formation, regarded as correlative to the Udurchukan Formation (Markevich and Bugdaeva 2001). Thus, these three taxa may be regarded as roughly contemporaneous. It is therefore legitimate to ask whether these are really three separate taxa. Table 2 summarises the main differences observed in their skeleton. Among the 22 characters listed here, 14 can be regarded as significantly different between *Amurosaurus riabinini* and *Charonosaurus jiayinensis*, fully justifying the generic separation between both taxa. The differences are less marked between *Olorotitan arharensis* and *Amurosaurus riabinini* (6 characters), but this is mainly because different parts of the skull are preserved in both taxa. The neurocranium and the skull roof are well-preserved in *Amurosaurus* and *Charonosaurus*, whereas we have no indications about the shape of the snout and supracranial crest. In *Olorotitan*, on the other hand, the snout and the supracranial crest have been discovered in connection, but the neurocranium and the skull roof remain unknown to date.

Phylogenetic relationships of *Amurosaurus riabinini*

In order to clarify the phylogenetic relationships of *Amurosaurus riabinini*, a parsimony analysis was carried out, based on 40 cranial, dental, and postcranial characters, and 11 hadrosauroid taxa. Because the monophyly of the hadrosaurid family and of the hadrosaurine and lambeosaurine subfamilies is accepted by the great majority of dinosaur specialists (see e.g., Weishampel and Horner 1990; Weishampel et al. 1993; Sereno 1998; Godefroit et al. 1998, 2001), all hadrosaurine genera are herein gathered into one single taxon labelled "Hadrosaurinae". The non-hadrosaurid Hadrosauroidea *Bactrosaurus johnsoni*, recently revised by Godefroit et al. (1998), has been chosen as the outgroup, because its anatomy is now particularly well-documented and familiar to the authors of the present paper. An exhaustive

Table 2. Differential characters between the three lambeosaurine taxa discovered in the Maastrichtian from the Amur region. Asterisk indicates a character state different from the condition encountered in *A. riabinini*.

Characters	***A. riabinini***	***C. jiayinensis***	***O. arharensis***
1. Horizontal groove on exoc.-opith. pillar	present	absent*	–
2. Median basipterygoid process	well developed	absent*	–
3. Alar process on basisphenoid	asymmetrical	very developed, symmetrical*	–
4. Paroccipital processes	long and pending	shortened*	–
5. Sagittal crest	very high caudally	not developed*	–
6. Participation of prefrontal in floor or supracranial crest	about 50%	no*	–
7. Proportions of frontals	longer than wide	wider than long*	–
8. Rostral platform of frontal	short	extends above supratemporal fenestra*	–
9. Caudal ramus of postorbital	very long, high and straight	slender and convex upwards*	–
10. Dosal surface of postorbital	flat	dorsal promontorium*	–
11. Medial processes of squamosals	separated by parietal	meeting in midline of occiput*	–
12. Rostral process of jugal	rounded	rounded	truncated, straight*
13. Height of postorbital process of jugal	jugal much longer than high	jugal much longer than high	L/H ratio = 0.9*
14. Ventral margin of maxilla	Straight	Straight	down-turned*
15. Lateral profile of maxilla	slightly asymmetrical	slightly asymmetrical	very asymmetrical*
16. Maxillary shelf	not very developed	–	very developed*
17. Number of sacral vertebrae	–	9	15 or 16
18. Radius and ulna	moderately elongated, sigmoidal	very elongated, straight*	–
19. Scapular blade	4.5<L/W ratio<5	4.5<L/W ratio<5	L/W ratio = 6.2 *
20. Ilium length / preacetabular length	–	>2.1	<2
21. Distal end of fibula	moderately expanded	club-shaped*	moderately expanded
22. Cranial ascending process of astragalus	skewed laterally	equilateral*	skewed laterally

search for all possible tree topologies was performed using PAUP*4.0b10 program (Swofford 2000), with both accelerated transformation (ACCTRAN) and delayed transformation (DELTRAN) options. The characters used in the present analysis are described and discussed in Appendix 1, the data matrix is presented in Appendix 2, and a complete list of apomorphies is found in caption to Fig. 19. PAUP analyses produced a single most parsimonious tree, with a length of 46 steps, a consistency index (CI) of 0.98 and a retention index (RI) of 0.96 (Fig. 19).

Hadrosauridae (*sensu* Sereno 1998), is supported by 13 "unambiguous" (no differences in positioning of a character in ACTRAN and DELTRAN optimizations) synapomorphies (characters 15, 19, 21, 24, 25, 26, 27, 28, 30, 33, 34, 36, 37; see Appendix 1 for description). With the exception of character 33 (more than 8 sacral vertebrae: there is no complete sacrum in the studied material), all these synapomorphies can be observed in *Amurosaurus riabinini*. The monophyly of the hadrosaurine subfamily is supported by 6 "unambiguous" synapomorphies (characters 8, 10, 12, 22, 32, and 38(2)). The lambeosaurine subfamily is supported by 9 "unambiguous" synampomorphies (characters 2, 3, 5, 16, 20, 23, 31, 35, and 38(1)); all can be observed in *Amurosaurus riabinini*. The absence of premaxillary foramina (character 7) and the external naris surrounded only by the premaxilla (character 11) are herein regarded as "ambiguous" synapomorphies for Lam-

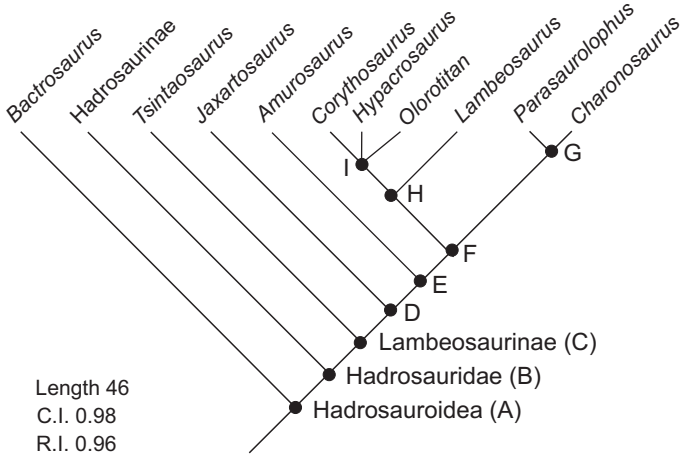

Fig. 19. Cladogram of Lambeosaurinae, showing the phylogenetic relationships of *Amurosaurus riabinini*. List of apomorphies for all ingroup taxa. Letters indicate nodes. For multistate characters, the number between brackets refers to the character state (see Appendix 1). Character are followed by an "a", when supported only by ACCTRAN or fast optimisation, and by a "d", when supported only by DELTRAN, or slow optimisation. Node A (Hadrosauridae): 15, 19, 21, 24, 25, 26, 27, 28, 30, 33, 34, 36, 37; Node B (Hadrosaurinae): 8, 10, 12, 22, 32, 38(2); Node C (Lambeosaurinae): 2, 3, 5, 7a, 11a, 16, 20, 23, 31, 35, 38(1); Node D: 4(1); Node E: 18; Node F: 6, 7d, 11d; Node G (parasauroloph clade, named according to Chapman and Brett-Surman 1990): 1, 4(2), 17, 39, 40; Node H (corythosaur clade, named according to Chapman and Brett-Surman 1990): 9, 13; Node I: 14(1).

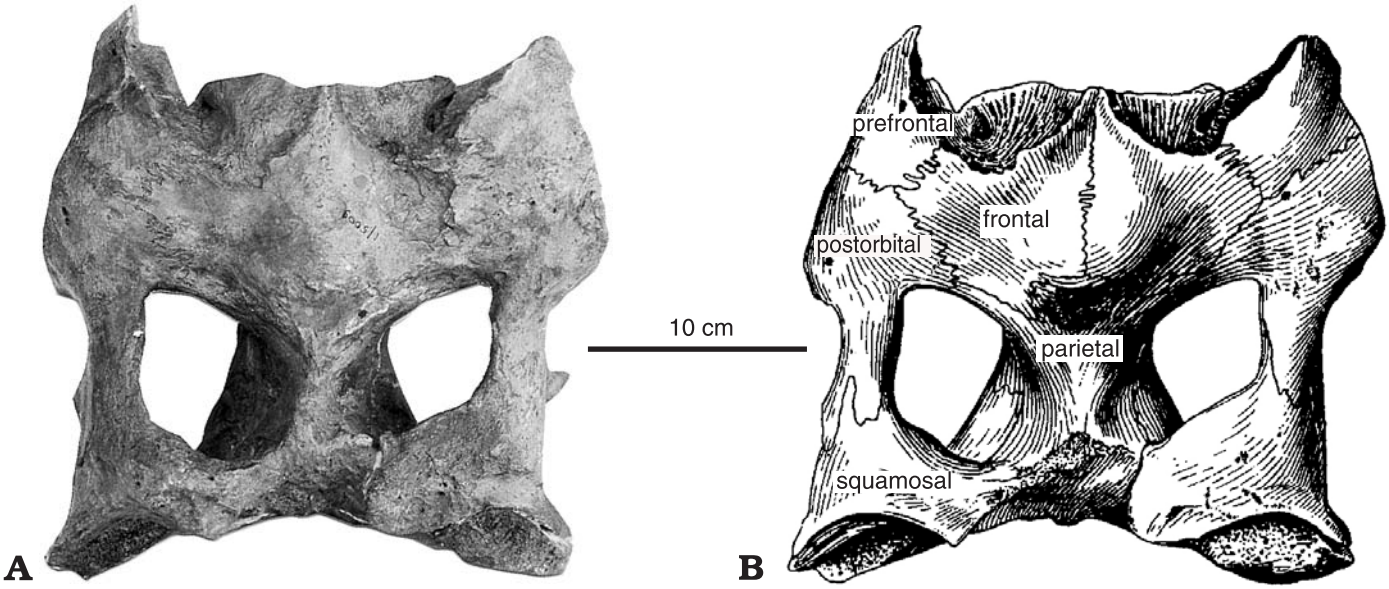

Fig. 20. Skull of *Jaxartosaurus aralensis* Riabinin, 1939 in dorsal view. **A**: PIN 1/5009; **B**, after Norman and Sues (2000).

beosaurinae, because these character cannot be observed in *Tsintaosaurus*, *Jaxartosaurus* and *Amurosaurus*, in which the premaxillae are not preserved. This analysis successively places these three taxa as the most basal Lambeosaurinae. *Tsintaosaurus* lacks the presence of a deeply excavated frontal platform (character 4(1)), which characterises all other Lambeosaurinae. The phylogenetic position of *Jaxartosaurus* is discussed in detail below; in this genus, the squamosal is not very elevated (character 18), as in more advanced Lambeosaurinae. *Amurosaurus* also occupies a basal position in lambeosaurine phylogeny: whereas its frontal is deeply excavated and its squamosal is elevated, its frontal is still relatively long. *Amurosaurus* is the siter-taxon of a monophyletic group formed by the parasauroloph and the corythosaur clades (named according to Chapman and Brett-Surman 1990). Both clades share a shortened frontal (character 6(1)), but also the two "ambiguous" synapomorphies discussed above (characters 7 and 11). The parasauroloph clade is supported by 5 "unambiguous" synapomorphies (characters 1, 4(2), 17, 39, 40) and the corythosaur clade, by 2 "unambiguous" synapomorphies (characters 9 and 13).

Remarks on the phylogenetic position of *Jaxartosaurus aralensis*

From 1923 to 1926, the Geological Committee of the USSR excavated the Kyrk-Kuduk dinosaur locality in the Chuley region of Chimkent/Tashkent in eastern Kazakhstan. Most of the fossils were discovered within a conglomerate that may be Santonian in age (Averianov and Nessov 1995). Riabinin (1939) described two hadrosaurid taxa from this locality: *Jaxartosaurus aralensis* and *Bactrosaurus prynadai*. *Bactrosaurus prynadai* is based on two dentaries and one maxilla belonging to juvenile individuals. This taxon is unanimously regarded as a *nomen dubium* (Maryańska and Osmólska 1981a; Weishampel and Horner 1990). *Jaxartosaurus aralensis* was described from the caudal part of one skull, one dentary, one surangular and a few postcranial elements. Unfortunately, it cannot be asserted whether these fossils were really found in association, or were dispersed within the bone-bed. The caudal part of the skull is now preserved in the Palaeontological Institute of the Russian Academy of Sciences at Moscow (PIN 1/5009; Fig. 20); the rest of the material is apparently lost (Vladimir R. Alifanov personal communication 2002). Rozhdestvensky (1968) accurately described this specimen in detail, so it is not necessary to do so again. We only would like to provide information about the phylogenetic position of this taxon, based on a few anatomical observations at hand.

Jaxartosaurus aralensis is unquestionably a member of Lambeosaurinae, because it displays the following synapomorphies of this subfamily: the frontal-prefrontal region is excavated to form a base for the hollow crest and the parietal is short, with a length/minimal width ratio < 2; moreover, the frontals form a well developed median bulge, as usually observed in juvenile lambeosaurines.

We consider that *Jaxartosaurus aralensis* is a valid taxon that cannot be synonymised with any other known lambeosaurine, because it displays the following autapomorphies: the lateral bar of the supratemporal fenestra is short and extremely robust, and the prootic process of the laterosphenoid is particularly thickened.

Jaxartosaurus aralensis probably holds a basal position in lambeosaurine phylogeny. The lateral border of its squamosal is not elevated above the cotylus (character 18 in Ap-

pendix 1), as observed in "corythosaurs", "parasaurolophs", and *Amurosaurus*; this primitive condition is also retained in *Tsintaosaurus*. Moreover, the excavated rostral portion of the frontal is proportionally shorter and shallower than in other Lambeosaurinae, except of course in *Tsintaosaurus*, in which it is not developed at all. Taking these elements into consideration, it is logical that *Jaxartosaurus* constitutes the sister group of the clade formed by the corythosaur clade + the parasauroloph clade + *Amurosaurus*. (Fig. 20). *Tsintaosaurus* therefore becomes the sister group of the clade fomed by *Jaxartosaurus* + higher lambeosaurines.

Riabinin (1939: pl. 8: 1, pl. 9: 1) referred a fragmentary left humerus to *Jaxartosaurus aralensis*. This humerus is particularly narrow and does not exhibit an enlarged deltopectoral crest, a synapomorphic feature for all Lambeosaurinae including *Tsintaosaurus* (see Young 1958: fig. 23). The problem remains as to whether this humerus, now lost, has really been associated with the holotype skull of *Jaxartosaurus aralensis*, or whether it belongs to a contemporary hadrosaurine. If the first hypothesis is confirmed, it means that *Jaxartosaurus*, *Tsintaosaurus*, and higher lambeosaurines form an unresolved tritomy in the current state of our knowledge.

It is also interesting to observe that the prefrontal takes a large part in the formation of the depressed base for the hollow crest in *Jaxartosaurus aralensis*, as in *Amurosaurus riabinini*. Because it is herein assumed that *Jaxartosaurus aralensis* is a basal lambeosaurine, it may therefore be hypothesised that this condition is plesiomorphic in lambeosaurines and that the more or less complete exclusion of the prefrontal from the base of the hollow crest, as observed for example in *Corythosaurus*, is on the other hand apomorphic. However, this hypothesis needs to be confirmed by future investigations. For that reason it was not taken into consideration in the phylogenetic analysis presented in this paper.

Palaeobiogeographical implications

The results of the cladistic analysis are also interesting from a palaeobiogeographical point of view. Norell (1992) defined ghost lineages as missing sections of a clade implied by phylogeny. As sister taxa have the same time of origin, it is therefore possible to establish the minimal age for the origin of clades: the origin of a clade cannot occur later than the first occurrence of its sister taxon. Ghost lineage duration can be calibrated using a geochronological scale: for sister taxa, it is the difference between the first occurrence of the younger taxon and the first occurrence of the older one.

Fig. 21 represents the ghost lineages identified for the taxa in our cladistic analysis. Asian taxa names are underlined. This figure clearly demonstrates that the most basal lambeosaurine dinosaurs come from Asian localities. These are successively *Tsintaosaurus spinorhinus*, from the Wangshi Series of Shandong Province in eastern China (Campanian, according to Buffetaut and Tong-Buffetaut 1993), *Jaxartosaurus aralensis*, from the Syuksyuk Formation of Kazakhstan (Santonian, according to Averianov and Nessov 1995), and *Amurosaurus riabinini*, from the Tsagayan Formation of the Amur region. In the current state of our knowledge, it may therefore be asserted that lambeosaurines originated in Asia. All the North American lambeosaurines described to date belong to the advanced corythosaur and parasauroloph clades. In this area, the oldest well-dated and well-identified lambeosaurines have been discovered in upper Campanian formations (Weishampel and Horner 1990), which means that lambeosaurines migrated toward western North America before or at the beginning of the late Campanian. During most of the Late Cretaceous, an interior seaway divided North America into a western Cordilleran region and an eastern shield region. A land route between Asian and Cordilleran America across the Beringian isthmus probably opened during the Aptian–Albian and persisted during the Late Cretaceous. Jerzykiewicz and Russell (1991) and Russell (1993) showed that many vertebrate groups, originating from Asia, migrated toward western North America through this route by Campanian–Maastrichtian time. Besides Lambeosaurinae, this is apparently the case for the following dinosaur taxa: basal Neoceratopsia (Chinnery and Weishampel 1998), Ceratopsidae (Nessov and Kazny-

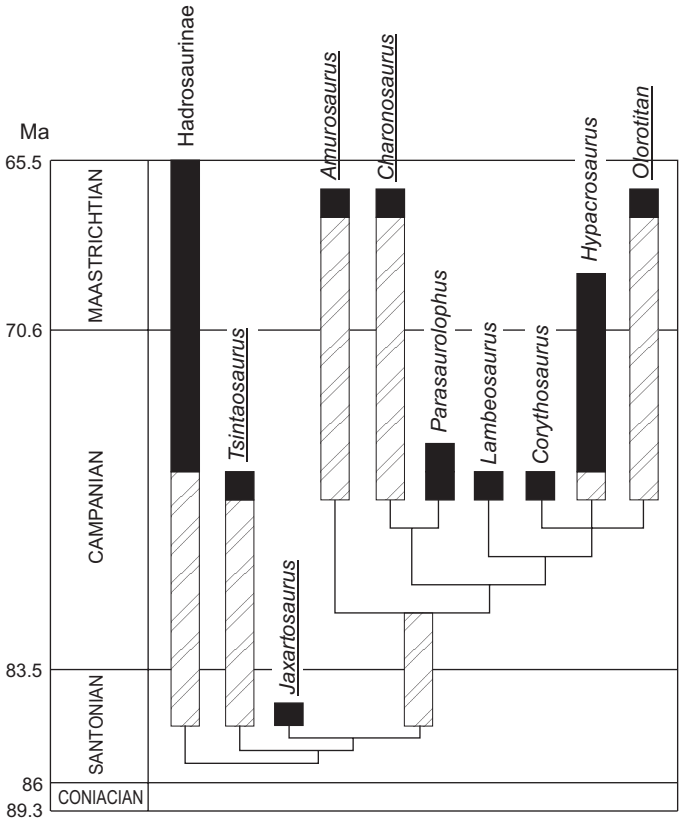

Fig. 21. Stratigraphically-calibrated cladogram of phylogenetic relationships of Lambeosaurinae, including *Amurosaurus*. Solid symbols indicate stratigraphical occurrence of a taxon, whereas hatched symbols indicate ghost lineages. Asian taxa are underlined. Dates are millions of years before present.

shkina 1989), Ankylosauridae (Maryańska 1977), Tyrannosauridae (Mader and Bradley 1989; Buffetaut et al. 1996), and Troodontidae (Russell and Dong 1993).

Fig. 21 also shows that, within advanced Lambeosaurinae, representatives of the corythosaur and parasauroloph clades have been discovered both in North America and in eastern Asia (Amur Region). It is therefore difficult to know exactly whether parasaurolophs and corythosaurs at first diversified in Asia and then independently migrated to North America or whether their common ancestors migrated before their diversification in North America. The second hypothesis appears at first sight more parsimonious, because *Lambeosaurus*, herein regarded as the most basal corythosaur, is a North American taxon. The age distribution of the taxa rather speaks in favour of the second interpretation too: in western North America, corythosaur and parasauroloph lambeosaurines are late Campanian or early Maastrichtian in age, whereas they are herein regarded as late Maastrichtian in age in the Amur region. This interpretation implies two independant secondary migrations from North America to Asia (*Olorotitan* and *Charonosaurus*). On the other hand, Jerzykiewicz and Russell (1991) and Russell (1993) observed that no dinosaur family is known to have originated in North America and then migrated to Asia. But the study of a new hadrosaurine from Blagoveschensk locality also implies a migration from east to west before the late Maastrichtian (Bolotsky and Godefroit 2004).

It therefore may be concluded that, even though the Beringian isthmus was situated in the polar region, many faunal exchanges occurred between Asia and western North America, so that both regions seem to have been effectively merged from a biogeographical point of view by Campanian–Maastrichtian time. Although the major direction of migration for dinosaurs seems to have been from Asia to western North America, several independent hadrosaurid lineages crossed the Beringian isthmus from east to west.

As previously noted by Godefroit et al. (2000, 2001), Maastrichtian dinosaur faunas from the Amur region are completely different from potentially synchronous Lancian faunas from western North America. Ceratopsian herbivorous dinosaurs, including *Triceratops*, *Torosaurus*, and *Leptoceratops* (Lehman 1987; Russell and Manabe 2002) usually dominate the latter. Hadrosauridae are also usually well-represented by members of the edmontosaur clade (*Edmontosaurus* and *Anatotitan*). The "titanosaurid" sauropod *Alamosaurus* also characterises Lancian dinosaur assemblages in Utah, New Mexico, Colorado, and Texas. Lambeosaurinae apparently disappeared from western North America by late Maastrichtian time, or are represented only by scarce and doubtful material (Boyd and Ott 2002). On the other hand, lambeosaurines dominate Maastrichtian dinosaur localities from the Amur region, where ceratopsians and "titanosaurids" are apparently not represented.

The development of different kinds of dinosaur communities during the late Maastrichtian may reflect either some kind of geographic isolation between eastern Asia and western North America during this period, or important differences in climatic or palaeoecological conditions. According to Markevich and Bugdaeva (1997), the Maastrichtian dinosaurs from the Amur region lived in savannah-like valleys with oasis vegetation along the banks of lakes and river, under a warm-temperate and relatively arid climate. Johnson (2002) showed that the Hell Creek Formation of the Dakotas was a forested environment, similar in appearance to a living mixed deciduous and evergreen broad-leafed forest. According to Russell and Manabe (2002), the absence of lambeosaurines in the Hell Creek Formation could be taken as evidence of uniform coastal wetland environment, usually avoided by these animals. However, the Lancian localities from western North America represent a relatively wide geographic-environmental range, including coastal lowlands, alluvial plains and piedmont lithosomes. Lambeosaurines are apparently absent from all of these different palaeoenvironments in western North America.

The present analysis is based on the assumption that the Blagoveschensk locality is late Maastrichtian in age, a hypothesis that still needs to be corroborated by further palynological analyses. Therefore, the observed differences between the Maastrichtian dinosaur faunas from the Amur region and the "Lancian" faunas from western North America may reflect temporal ambiguity rather than spatial differenciation.

Acknowledgements

Although the first dinosaur fossils from the Amur region were discovered a century ago, real exploration of dinosaur localities really began in the beginning of the 1980s, when AmurKNII was created. From the first day, this work was led by Academican Valentin G. Moiseenko. Hard field work became easier owning to the priceless help of many good friends: first of all Michail Gerasimov, Dmitri Klokov, Anatoli Samokrutov, Alona Komarova, Nikolai Melnikov, and Dmitri Baranov. Valentina Markevich and Evgenia Bugdaeva (Biological and Pedological Institute, Vladivostok) regularly took part in our field work and helped to clarify the problems related to the age and palaeoenvironment of the dinosaur beds. Many specialists gave us helpful advices and provided literature: Sergei M. Kurzanov, Alexander S. Rautian, Nikolai N. Kalandadze, Vladimir R. Alifanov, and Evgeni N. Kurochkin (Palaeontological Institute, Moscow), and the late Lev A. Nessov and Alexander O. Averianov (St. Petersbourg). We also want to thank very much the workers at the Palaeontological Museum of Amur KNII who spent so much time and energy for this exploration: Alexander A. Kotov, Sergei A. Karev, Nathalia Bolotskaya, and Ivan Y. Bolotsky. This study was realised through the execution of Science & Technology bilateral cooperation agreements on behalf of the Belgian State, Federal Scientific Policy. Excavations in Blagoveschensk locality were partly supported by the Jurassic Fundation. P.G.'s travels in Amur Region were partly covered by a travel grant from the Fonds National de la Recherche Scientifique. P.G. would like to thank Evgeni N. Kurochkin and Vladimir R. Alifanov (Palaeontological Institute, Moscow), and Eugene S. Gaffney and Mark A. Norell (AMNH, New York) who facilitated access to material in their care. He is also particularly grateful to Olga Scherbinina for help in translation, and to Nathalia Bolotskaya for cordial hospitality during his numerous stays at Blagoveschensk. Drawings were made by Ann Wauters. David B. Norman and David B. Weishampel reviewed the manuscript of this paper and made many very helpful comments.

References

Alifanov, V.R. and Bolotsky, Y.L. 2002. New data about the assemblages of the Upper Cretaceous carnivorous dinosaurs (Theropoda) from the Amur Region. *In*: G.L. Kirillova (ed.), *Cretaceous Continental Margin of East Asia: Stratigraphy, Sedimentation, and Tectonics*, 25–26. UNESCO-IUGS-IGCP, Khabarovsk.

Averianov, A. and Nessov, L. 1995. A new Cretaceous mammal from the Campanian of Kazakhstan. *Neues Jahrbuch für Geologie und Paläontologie, Monatshefte* 1995: 65–74.

Bolotsky, Y.L. [Bolockij, Û.L.] and Kurzanov, S.K. 1991. The hadrosaurs of the Amur Region [in Russian]. *In*: *Glubinnoe Stroenie Tihookeanskogo Obranleniâ*, 94–103. Amur KNII, Blagoveŝensk.

Bolotsky, Y.L. and Godefroit, P. 2004. A new hadrosaurine dinosaur from the Late Cretaceous of Far Eastern Russia. *Journal of Vertebrate Palaeontology* 24 (2): 354–368.

Boyd, C. and Ott, C.J. 2002. Probable lambeosaurine (Ornithischia, Hadrosauridae) specimen from the Late Cretaceous Hell Creek Formation of Montana. *Journal of Vertebrate Paleontology* 22 (Supplement to No 3): 38A.

Braman, D.R. and Sweet, A.R. 1999. Terrestrial palynomorph biostratigraphy of the Cypress Hills, Wood Formation, and Turtle Mountain areas (Upper Cretaceous–Paleocene) of western Canada. *Canadian Journal of Earth Sciences* 36: 725–741.

Brett-Surman, M.K. 1989. *A Revision of the Hadrosauridae (Reptilia: Ornithischia) and Their Evolution During the Campanian and Maastrichtian*. 272 pp. Unpublished Ph.D. thesis, George Washington University, Washington DC.

Buffetaut, E., Suteethorn, V., and Tong, H. 1996. The earliest known tyrannosaur from the Lower Cretacous of Thailand. *Nature* 381: 689–691.

Buffetaut, E. and Tong-Buffetaut, H. 1993. *Tsintaosaurus spinorhinus* Young and *Tanius sinensis* Wiman: a preliminary comparative study of two hadrosaurs (Dinosauria) from the Upper Cretaceous of China. *Comptes rendus de l'Académie des Sciences, série 2,* 317 (9): 1255–1261.

Bugdaeva, E.V., Markevich, V.S. [Markevič, V.S.], Bolotsky, Y.L. [Bolockij, Û.L.], and Sorokin, A.P. 2000. Extinction of dinosaurs in Cretaceous period: paleobotanists' view [in Russian]. *Vestnik Dal'nevostočnogo Otdeleniâ Rossijskoj Akademii Nauk* 1: 80–88.

Casanovas, M.L., Pereda Suberbiola, X., Santafe, J.V., and Weishampel, D.B. 1999. A primitive euhadrosaurian dinosaur from the uppermost Cretaceous of the Ager syncline (southern Pyrenees, Catalonia). *Geologie en Mijnbouw* 78: 345–356.

Chapman, R.E. and Brett-Surman, M.K. 1990. Morphometric observations on hadrosaurid ornithopods. *In*: K. Carpenter, K.F. Hirsch, and J.R. Horner (eds.), *Dinosaur Eggs and Babies*, 163–177. Cambridge University Press, Cambridge.

Chinnery, B.J. and Weishampel, D.B. 1998. *Montanoceratops cerorhynchus* (Dinosauria: Ceratopsia) and relationships among basal neoceratopsians. *Journal of Vertebrate Paleontology* 18 (3): 569–585.

Cope, E.D. 1869. Synopsis of the extinct Batrachia, Reptilia and Aves of North-America. *Transactions of the American Philosophical Society* 14: 1–252.

Galton, P.M. 1974. The ornithischian dinosaur *Hypsilophodon* from the Wealden of the Isle of Wight. *Bulletin of the British Museum (Natural History), Geology* 25 (1): 1–152.

Gilmore, C.W. 1924a. On the genus *Stephanosaurus*, with a description of the type specimen of *Lambeosaurus lambei* Parks. *Bulletin of the Canada Department of Mines and Geological Survey* 38: 29–48.

Gilmore, C.W. 1924b. On the skull and skeleton of *Hypacrosaurus*, a helmet-crested dinosaur from the Edmonton Cretaceous of Alberta. *Bulletin of the Canada Department of Mines and Geological Survey* 38: 49–64.

Gilmore, C. W. 1933. On the dinosaurian fauna of the Iren Dabasu Formation. *Bulletin of the American Museum of Natural History* 67: 23–78.

Gilmore, C.W. 1937. On the detailed skull structure of a crested hadrosaurian dinosaur. *Proceedings of the United States National Museum* 84: 481–491.

Godefroit, P., Dong, Z.-M., Bultynck, P., Li, H., and Feng, L. 1998. New *Bactrosaurus* (Dinosauria: Hadrosauroidea) material from Iren Dabasu (Inner Mongolia, P.R. China). *Bulletin de l'Institut royal des Sciences naturelles de Belgique, Sciences de la Terre* 68 (Supplement): 3–70.

Godefroit, P., Zan, S., and Jin, L. 2000. *Charonosaurus jiayinensis* n.g., n.sp., a lambeosaurine dinosaur from the Late Maastrichtian of north-eastern China. *Comptes rendus de l'Académie des Sciences de Paris, Sciences de la Terre et des Planètes* 330: 875–882.

Godefroit, P., Zan, S., and Jin, L. 2001. The Maastrichtian (Late Cretaceous) lambeosaurine dinosaur *Charonosaurus jiayinensis* from north-eastern China. *Bulletin de l'Institut royal des Sciences naturelles de Belgique, Sciences de la Terre* 71: 119–168.

Godefroit, P., Bolotsky, Y.L., and Alifanov, V. 2003. A remarkable hollow-crested hadrosaur from Russia: an Asian origin for lambeosaurines. *Comptes Rendus Palevol* 2: 143–151.

Herngreen, G.F.W. and Chlonova, A.F. 1981. Cretaceous microfloral provinces. *Pollen et Spores* 23 (3–4): 441–555.

Herngreen, G.F.W., Kedves, M., Rovnina, L.V., and Smirnova, S.B. 1996. Cretaceous palynofloral provinces: a review. *In*: J. Jansonius and D.C. McGregor (eds.), *Palynology: Principles and Applications*, 1157–1188. American Association of Stratigraphic Palynologists Foundation, Dallas.

Horner, J.R. 1990. Evidence of diphyletic origination of the hadrosaurian (Reptila: Ornithischia) dinosaurs. *In*: K. Carpenter and P.J. Currie (eds.), *Dinosaur Systematics, Approaches and Perspectives*, 179–187. Cambridge University Press, Cambridge.

Horner, J.R. 1992. Cranial morphology of *Prosaurolophus* (Ornithischia: Hadrosauridae) with description of two new hadrosaurid species and an evaluation of hadrosaurid phylogenetical relationships. *Museum of the Rockies Occasional Paper* 2: 1–119.

Horner, J.R. and Currie, P.J. 1994. Embryonic and neonatal morphology and ontogeny of a new species of *Hypacrosaurus* (Ornithischia, Lambeosauridae) from Montana and Alberta. *In*: K. Carpenter, K.F. Hirsch, and J.R. Horner (eds.), *Dinosaur Eggs and Babies*, 312–336. Cambridge University Press, Cambridge.

Jerzykiewicz, T. and Russell, D.A. 1991. Late Mesozoic stratigraphy and vertebrates of the Gobi Basin. *Cretaceous Research* 12: 345–377.

Johnson, K.R. 2002. Megaflora of the Hell Creek and Fort Union Formations in the western Dakotas: vegetational response to climate change, the Cretaceous–Tertiary boundary event, and rapid marine trangression. *In:* J.H. Hartman, K.R. Johnson, and D.J. Nichols (eds.), The Hell Creek Formation and the Cretaceous–Tertiary Boundary in the Northern Great Plains: An Integrated Continental Record of the End of the Cretaceous. *Geological Society of America, Special Paper* 361: 329–391.

Kirillova, G.L., Markevich, V.S., and Bugdaeva, E.V. 1997. Correlation of geologic events in the Cretaceous basins of Southeast Russia. *Geology of Pacific Ocean* 13: 507–526.

Kirkland, J.J. 1998. A new hadrosaurid from the Upper Cedar Mountain Formation (Albian–Cenomanian: Cretaceous) of eastern Utah—the oldest known hadrosaurid (lambeosaurine?). *New Mexico Museum of Natural History and Science* 14: 283–302.

Lambe, L.M. 1920. The hadrosaur *Edmontosaurus* from the Upper Cretaceous of Alberta. *Memoirs of the Canada Department of Mines and Geological Survey* 120: 1–79.

Lerbekmo, J.F., Sweet, A.R., and Louis, R.M.S. 1987. The relationship between the iridium anomaly and palynological floral events at three Cretaceous–Tertiary boundary localities in western Canada. *Geological Society of America Bulletin* 99: 325–330.

Leffingwell, H.A. 1970. Palynology of the Lance (Late Cretaceous) and Fort Union (Paleocene) Formations of the type Lance area, Wyoming. *Geological Society of America Special Paper* 127: 1–64

Lehman, T.M. 1987. Late Maastrichtian paleoenvironments and dinosaur biogeography in the western interior of North America. *Palaeogeography, Palaeoclimatology, Palaeoecology* 60: 189–217.

Mader, B.J. and Bradley, R.L. 1989. A redescription and revised diagnosis of the syntypes of the Mongolian tyrannosaur *Alectrosaurus olseni*. *Journal of Vertebrate Paleontology* 9: 41–55.

Markevich, V.S. 1994. Palynological zonation of the continental Cretaceous and early Tertiary of eastern Russia. *Cretaceous Research* 15: 165–177.

Markevich, V.S. [Markevič, V.S.] and Bugdaeva, Y.V. 1997. Flora and correlation of layers with dinosaur fossil remains in Russia's Far East [in Russian]. *Tihookeanskaâ Geologiâ* 16: 114–124.

Markevich, V.S. [Markevič, V.S.] and Bugdaeva, E.V. 2001. Correlation of the Upper Cretaceous and Palaeogene plant-bearing deposits of the Russian Far East [in Russian]. *In:* E.V. Bugdaeva (ed.), *Flora i dinozavry na granice mela i paleogena Zejsko-Bureinskogo Bassejna*, 79–96. Dal'nauka, Vladivostok.

Marsh, O.C. 1881. Classification of the Dinosauria. *American Journal of Science, series 3*, 23: 81–86.

Maryańska, T. 1977. Ankylosauridae (Dinosauria) from Mongolia. *Palaeontologica Polonica* 30: 85–151.

Maryańska, T. and Osmólska, H. 1979. Aspects of hadrosaurian cranial anatomy. *Lethaia* 12: 265–273.

Maryańska, T. and Osmólska, H. 1981a. Cranial anatomy of *Saurolophus angustirostris* with comments on the Asian Hadrosauridae (Dinosauria). *Palaeontologia Polonica* 42: 5–24.

Maryańska, T. and Osmólska, H. 1981b. First lambeosaurine dinosaur from the Nemegt Formation. *Acta Palaeontologica Polonica* 26: 243–255.

Nessov, L.A. [Nesov, L.A.] and Kaznyshkina, F. [Kaznyškina, F.] 1989. Ceratopsian dinosaurs and crocodiles of the middle Mesozoic of Asia [in Russian]. *In*: T.N. Bogdanova and L.I. Hozackij (eds.), *Trudy 33 Sessii Vsesoûznogo Paleontologičeskogo Obŝestva*, 142–149. Nauka, Leningrad.

Newman, K.R. 1987. Biostratigraphic correlation of Cretaceous–Tertiary boundary rocks, Colorado to San Juan Basin, New Mexico. *Geological Society of America Special Papers* 209: 151–164.

Nichols, D.J. 2002. Palynology and biostratigraphy of the Hell Creek Formation in North Dakota: a microfossil record of plants at the end of Cretaceous time. *In:* J.H. Hartman, K.R. Johnson, and D.J. Nichols (eds.), The Hell Creek Formation and the Cretaceous–Tertiary Boundary in the Northern Great Plains: An Integrated Continental Record of the End of the Cretaceous. *Geological Society of America, Special Paper* 361: 393–456.

Nichols, D.J., Jarzen, D.M., Orth, C.J., and Oliver, P.Q. 1986. Palynological and iridium anomalies at the Cretaceous–Tertiary boundary, South-Central Saskatchewan. *Science* 231: 714–717.

Nichols, D.J. and Sweet, A.R. 1993. Biostratigraphy of Upper Cretaceous non-marine palynofloras in a north-south transect of the Western Interior Basin. *In*: W.G.E. Caldwell and E.G. Kauffman (eds.), Evolution of the Western Interior Basin. *Geological Association of Canada, Special Paper* 39: 539–584.

Norell, M.A. 1992. Taxic origin and temporal diversity: the effect of phylogeny. *In*: M. Novacek and Q. Wheelers (eds.), *Extinction and Phylogeny*, 89–118. Columbia University Press, New York.

Norman, D.B. 1980. On the ornithischian dinosaur *Iguanodon bernissartensis* of Bernissart (Belgium). *Mémoires de l'Institut royal des Sciences naturelles de Belgique* 178: 1–103.

Norman, D.B. 1984. On the cranial morphology and evolution of ornithopod dinosaurs. *Symposium of the Zoological Society of London* 5: 521–547.

Norman, D.B. 1986. On the anatomy of *Iguanodon atherfieldensis* (Ornithischia, Ornithopoda). *Bulletin de l'Institut royal des Sciences naturelles de Belgique, Sciences de la Terre* 56: 281–372.

Norman, D.B. 1998. On Asian ornithopods (Dinosauria: Ornithischia). 3. A new species of iguanodontid dinosaur. *Zoological Journal of the Linnean Society* 122: 291–348.

Norman, D.B. and Sues, H.-D. 2000. Ornithopods from Kazakhstan, Mongolia and Siberia. *In*: M.J. Benton, M.A. Shishkin, D.M. Unwin, and E.N. Kurochkin (eds.), *The Age of Dinosaurs in Russia and Mongolia*, 462–479. Cambridge University Press, Cambridge.

Ostrom, J.H. 1961. Cranial morphology of the hadrosaurian dinosaurs of North America. *Bulletin of the American Museum of natural History* 122 (2): 33–186.

Owen, R. 1842. Report on British fossil reptiles. Part II. *In*: *Report of the Eleventh Meeting of the British Association for the Advancement of Science, held at Plymouth, July 1841*, 66–204. London.

Parks, W.A. 1922. *Parasaurolophus walkeri*, a new genus and species of crested trachodont dinosaur. *University of Toronto Studies, Geological Series* 13: 1–32.

Parks, W.A. 1923. *Corythosaurus intermedius*, a new species of trachodont dinosaur. *University of Toronto Studies, Geological Series* 15: 5–57.

Riabinin, A.N. [Râbinin, A.N.] 1925. A mounted skeleton of the gigantic reptile *Trachodon amurense* nov. sp. [in Russian]. *Izvestiâ Geologičeskogo Komiteta* 44: 1–12.

Riabinin A.N. [Râbinin A.N.] 1930a. *Manschurosaurus amurensis* nov. gen. nov. sp., a hadrosaurian dinosaur from the Upper Cretaceous of Amur River [in Russian]. *Russkoe Paleontologičeskoe Obŝestvo, Monografiâ* 11: 1–36.

Riabinin, A.N. [Râbinin A.N.] 1930b. On the age and fauna of the dinosaur beds on the Amur River [in Russian]. *Zapiski Russkogo Mineralogičeskogo Obŝestva* 59: 41–51.

Riabinin, A.N. [Râbinin A.N.] 1939. The Upper Cretaceous vertebrate fauna of south Kazakhstan. I. Pt. 1. Ornithischia [in Russian]. *Centralnyj Naučno-issledovatelnyj geologičeskij Institut, Trudy* 118: 1–40.

Rozhdestvensky, A.K. [Roždestvenskij, A.K.] 1957. On the Upper Cretaceous dinosaur localities of the Amur River [in Russian]. *Vertebrata PalAsiatica* 1: 285–291.

Rozhdestvensky, A.K. [Roždestvenskij, A.K.] 1968. Hadrosaurs of Kazakhstan [in Russian]. *In*: L.P. Tatarinov et al. (eds.), *Verhnepaleozojskie i mezozojskie zemnovodnye i presmykaûŝiesâ SSSR*, 97–141. Akademiâ Nauk SSSR, Moskva.

Russell, D.A. 1993. The role of Central Asia in dinosaurian biogeography. *Canadian Journal of Earth Sciences* 30: 2002–2012.

Russell, D.A and Dong, Z.-M. 1993. A nearly complete skeleton of a new troodontid dinosaur from the Early Cretaceous of the Ordos Basin, Inner Mongolia, People's Republic of China. *Canadian Journal of Earth Sciences* 30: 2163–2173.

Russell, D.A. and Manabe, M. 2002. Synopsis of the Hell Creek (uppermost Cretaceous) dinosaur assemblage. *In:* J.H. Hartman, K.R. Johnson, and D.J. Nichols (eds.), The Hell Creek Formation and the Cretaceous–Tertiary Boundary in the Northern Great Plains: An Integrated Continental Record of the End of the Cretaceous. *Geological Society of America, Special Paper* 361: 169–176.

Seeley, H.G. 1887. On the classification of the fossil animals commonly called Dinosauria. *Proceedings of the Royal Society of London* 43: 165–171.

Sereno, P.C. 1986. Phylogeny of the bird-hipped dinosaurs (Order Ornithischia). *National Geographic Research* 2: 234–256.

Sereno, P.C. 1998. A rationale for phylogenetic definitions, with application to the higher-level taxonomy of Dinosauria. *Neues Jahrbuch für Geologie und Paläontologie, Abhandlungen* 210 (1): 41–83.

Srivastava, S.K. 1970. Pollen biostratigraphy and paleoecology of the Edmonton Formation (Maestrichtian), Alberta, Canada. *Palaeogeography, Palaeoclimatology, Palaeoecology* 7: 221–276.

Sternberg, C.M. 1935. Hooded hadrosaurs of the Belly River Series of the Upper Cretaceous. *Bulletin of the Canada Department of Mines and Geological Survey* 77: 1–38.

Sullivan, R.M. and Williamson, T.E. 1999. A new skull of *Parasaurolophus* (Dinosauria: Hadrosauridae) from the Kirkland Formation of New Mexico and a revision of the genus. *New Mexico Museum of Natural History and Science* 15: 1–52.

Swofford, D.L. 2000. *Phylogenetic Analysis Using Parsimony (and other methods). Version 4.0b10*. 40 pp. Sinauer Associates, Sunderand, Massaschusetts.

Taquet, P. 1976. *Géologie et paléontologie du gisement de Gadoufaoua (Aptien du Niger).* 191 pp. Cahiers de Paléontologie, Centre national de la Recherche scientifique, Paris.

Weishampel, D.B. 1984. Evolution of jaw mechanisms in ornithopod dinosaurs. *Advances in Anatomy, Embryology and Cell Biology* 87: 1–110.

Weishampel, D.B., Dodson, P., and Osmólska, H. 1990. Introduction. *In*: D.B. Weishampel, P. Dodson, and H. Osmólska (eds.), *The Dinosauria*, 1–7. University of California Press, Berkeley.

Weishampel, D.B. and Horner, J.R. 1990. Hadrosauridae. *In*: D.B. Weishampel, P. Dodson, and H. Osmólska (eds.), *The Dinosauria*, 534–561. University of California Press, Berkeley.

Weishampel, D.B., Norman, D.B., and Grigorescu, D. 1993. *Telmatosaurus transsylvanicus* from the Late Cretaceous of Romania: the most basal hadrosaurid dinosaur. *Palaeontology* 36 (2): 361–385.

Young, C.C. 1958. The dinosaurian remains of Laiyang, Shantung. *Palaeontologia Sinica, series C* 16: 1–138.

Appendix 1

Characters and character states for determining the phylogenetic position of *Amurosaurus riabinini*. Most of those characters were previously discussed by Godefroit et al. (1998, 2001) and are therefore not described in detail in the present paper.

1. Parietal participating in the occipital aspect of the skull (0), or completely excluded from the occiput (1).
2. Ratio "length/minimal width" of the parietal > 2 (0), or < 2 (1).
3. Hollow supracranial crest absent (0), or present (1)—This is the most striking synapomorphy for Lambeosaurinae. Buffetaut and Tong-Buffetaut (1993) demonstrated that even *Tsintaosaurus spinorhinus* is characterised by such a hollow crest.
4. Deeply excavated frontal platform absent (0), occupying the rostral part of the frontal in adults (1), or extending above the rostral portion of the supratemporal fenestra (2). Character treated as ordered.
5. Frontal participating in the orbital rim (0), or excluded by post-orbital-prefrontal joint (1)—Maryańska and Osmólska (1979) showed that the frontal enters the orbital margin in flat-headed hadrosauroids such as *Bactrosaurus* (see also Godefroit et al. 1998), *Edmontosaurus*, and *Anatotitan*. However, the frontal of *Brachylophosaurus* and *Maiasaura*, which both bear solid crests, also participates along a short distance in the orbital rim (Albert Prieto-Marquez, personal communication July 2003). This is the plesiomorphic condition encountered in archosaurs. Exclusion of the frontal from the orbital rim is observed in all lambeosaurines, but also in some hadrosaurines, such as *Prosaurolophus* (see Horner 1992: pl. 38, B), *Kritosaurus* (see Horner 1992: pl. 44, B), and *Saurolophus* (see Maryańska and Osmólska 1981a). The situation remains unclear in *Gryposaurus*.
6. Frontal relatively long, with a "posterior length/maximal width" ratio > 0.75 (0), very shortened frontal, with a "posterior length/maximal width" < 0.6 (1), or secondary elongation resulting of the backward extension of the frontal platform (2). Character treated as ordered—Ancestrally in Iguanodontia, the frontal is distinctly longer (rostrocaudally) than wide (mediolaterally). This condition is observed not only in *Iguanodon*, *Bactrosaurus*, *Telmatosaurus*, and all Hadrosaurinae, but also in *Tsintaosaurus spinorhinus* (see Young 1958: fig. 1). Shortening of the frontal is obvious in advanced lambeosaurines. However, the length of the frontal is difficult to measure in lambeosaurines, because the very thin rostral part of the frontal platform is usually more or less broken. The posterior length of the frontal is a good estimate of its total length. The posterior length is the distance between the most caudal point of the frontal and the contact point between the frontal, the prefrontal and the postorbital, parallel to the sagittal axis of the skull roof. This measurement is therefore independent from the development of the rostral platform. The maximal width of the frontal is the distance between the contact point between the frontal, the prefrontal and the postorbital, and the medial border of the frontal, perpendicular to the sagittal axis of the skull roof. The posterior part of the frontal remains relatively long in *Jaxartosaurus aralensis* and *Amurosaurus riabinini* (1.02 in AEHM 1/232). In *Corythosaurus casuarius* (see Ostrom 1961), *Lambeosaurus* sp. (see Gilmore 1924a), *Hypacrosaurus altispinus* (see Gilmore 1924b), and *Charonosaurus jiayinensis* (see Godefroit et al. 2001), on the other hand, the posterior part of the frontal is distinctly shorter, with a "posterior length/maximal width" ratio < 0.6. However, this character has an important ontogenetic component: immature individuals, in which the dorsal platform is not fully developped, keep a relatively long frontal. Consequently this character is only valid for mature individuals. The secondary elongation of the frontal in *Parasaurolophus tubicen* results in the development of the frontal platform extending backward above the supratemporal fenestra (Sullivan and Williamson 1999: fig. 9).
7. Premaxillary foramen present (0), or absent (1)—Ancestrally in Euornithopoda, premaxillary foramina lead to a canal between the narial fossa and the palatal surface of the premaxilla. Weishampel et al. (1993) regarded loss of these foramina as a synapomorphy for Lambeosaurinae, because they are absent in *Corythosaurus*, *Hypacrosaurus*, *Lambeosaurus*, and *Parasaurolophus*. They are also absent in *Olorotitan*.
8. Premaxillary rostrum relatively narrow (0), or laterally expanded (1)—The primitive condition is retained in *Bactrosaurus* and Lambeosaurinae. On the other hand, the rostrum is distinctly expanded in all Hadrosaurinae (Horner 1992; Weishampel et al. 1993).
9. Lateral premaxillary process stopping at the level of the lacrimal (0), or extending farther backward (1)—Among Lambeosaurinae, *Corythosaurus*, *Hypacrosaurus*, *Lambeosaurus*, and *Olorotitan* are characterised by a backward expansion of the lateral premaxillary process, which participates in the lateral wall of the supracranial crest. In *Parasaurolophus*, on the other hand, the lateral premaxillary process remains relatively short and stops at the level of the lacrimal. This is the primitive condition encountered in more basal euornithopods and in Hadrosaurinae.
10. External naris relatively small (0), or large (1)—According to Weishampel et al. (1993), the external naris is relatively large (up to 40 per cent of basal skull length) in all Hadrosaurinae, with the exception of *Maiasaura* (reversal). Primitively for Ankylopollexia, it is slightly more than 20 per cent of basal skull length, as observed in Lambeosaurinae.
11. External naris surrounded by both the nasal and premaxilla (0), or only by the premaxilla (1)—Ancestrally in Iguanodontia, the external naris is surrounded by the premaxilla on its rostral and ventral margins, whereas the dorsal and caudal margins are formed by the nasal. This condition can be observed in *Bactrosaurus* and Hadrosaurinae. On the other hand, the external naris is completely surrounded by the premaxilla in *Parasaurolophus*, *Corythosaurus*, *Hypacrosaurus*, *Lambeosaurus*, and *Olorotitan*.
12. Circumnarial depression absent (0), or extending onto the nasal (1)—The development of a faint to well developed circumnarial depression onto the nasal is usually regarded as one of the major hadrosaurine synapomorphies (Weishampel and Horner 1990; Horner 1992; Weishampel et al. 1993). This character is not de-

veloped in non-hadrosaurid Hadrosauroidea, such as *Bactrosaurus*. Because of the migration of the nasal cavity to a supracranial position, this character is also regarded as absent in Lambeosaurinae.

13. *Cavum nasi proprium* relatively small (0), or enlarged (1)—Using ontogenetic arguments, Weishampel and Horner (1990) and Weishampel et al. (1993) considered that the common median chamber of the hollow crest is relatively small primitively in Lambeosaurinae. In contrast, the chamber is distinctly much enlarged in *Corythosaurus*, *Hypacrosaurus*, and *Lambeosaurus*.
14. Nasal forming a small part of the hollow crest (0), half of the crest (1), or the entire crest (2). Character treated as unordered—Contrary to Weishampel et al. (1993) and Godefroit et al. (2001), the nasal forming half of the hollow crest is herein regarded as synapomorphic for *Corythosaurus*, *Hypacrosaurus*, and *Olorotitan*, whereas *Lambeosaurus* retains the plesiomorphic condition. If the tubular hollow crest of *Tsintaosaurus* is not an artefact, this structure is entirely formed by the nasals (see Buffetaut and Tong-Buffetaut 1993). However, the structure of the crest in this genus is so peculiar that, in any case, it cannot derive from a corythosaur— like crest. Therefore, we consider that the degree of participation of the nasal in the supracranial hollow crest must be treated as unordered.
15. Supraorbital free (0), or fused to the prefrontal (1)—The presence of supraorbitals is a primitive character in ornithopods, observed in *Bactrosaurus johnsoni*. Maryańska and Osmólska (1979) showed that in advanced Lambeosaurinae and Hadrosaurinae, the absence of supraorbital bones can be explained by their fusion with the prefrontals: in these taxa, the "prefrontal" is therefore a coalescence of the true prefrontals and supraorbitals. Additional supraorbitals fuse with the orbital margin of the frontals and sometimes with the postorbitals.
16. Caudal portion of the prefrontal oriented horizontally (0), or participating in the lateroventral border of the hollow crest (1).
17. Dorsal surface of postorbital flat (0), or thickened to form a dorsal promontorium (1)—This dorsal promontorium is developed in adults of *Charonosaurus* (see Godefroit et al. 2001: fig. 6) and *Parasaurolophus* (see Sullivan and Williamson 1999: figs. 16, 17). This character is directly related to the backward extension of the hollow supracranial crest (Godefroit et al. 2001).
18. Lateral side of the squamosal low (0), or elevated (1)—The squamosal of *Amurosaurus riabinini* resembles that of typical lambeosaurines in being markedly elevated above the cotyloid cavity. The ratio "maximal height of the median ramus of the squamosal/maximal height of the paroccipital process" > 1 is the condition encountered in *Corythosaurus* (see Ostrom 1961: fig. 12), *Lambeosaurus* (see Gilmore 1924a: pl. 6), *Hypacrosaurus* (see Gilmore 1924b: pl. 11), *Parasaurolophus* (see Parks 1922: pl. 3), and *Olorotitan* (see Godefroit et al. 2001: fig. 7). The dorsal part of the squamosal is primitively distinctly lower in Hadrosauriformes, as observed in *Bactrosaurus*, *Eolambia* (see Kirkland 1998: fig. 5a–c), *Edmontosaurus*, *Anatotitan*, *Prosaurolophus, Saurolophus*, *Brachylophosaurus*, *Maiasaura*, *Gryposaurus*, and *Tsintaosaurus*.
19. Rostral process of the jugal tapering in lateral view (0), or dorsoventrally expanded (1).
20. Rostral process of the jugal angular (0), round and symmetrical in lateral view (1), or rostral border straight (2)—Character treated as unordered.
21. Antorbital fenestra surrounded by the jugal and/or the lacrimal (0), or completely surrounded by the maxilla (1).
22. Maxilla markedly asymmetrical (0), or nearly symmetrical in lateral view (1).
23. Rostromedial process developed on the maxilla (0), or maxillary shelf developed (1)—In iguanodontids, *Bactrosaurus*, and Hadrosaurinae, a rostromedial maxillary process helps the rostrolateral process in supporting the premaxilla. In Lambeosaurinae, on the other hand, the rostromedial process is absent, but a broadened medial maxillary shelf supports the medial aspect of the maxilla-premaxilla contact (Horner 1990; Weishampel et al. 1993).
24. Ectopterygoid ridge faintly (0), or strongly (1) developed on the lateral side of the maxilla.
25. Paraquadratic foramen present (0), or absent (1).
26. Ventral end of the quadrate transversely expanded (0), or dominated by a large hemispheric lateral condyle (1).
27. Mandibular diastema absent (0), or well developed in adults (1).
28. Coronoid process subvertical (0), or inclined rostrally (1).
29. Predentary round (0), or angular (1) in dorsal view—The rostral margin of the scoop-shaped predentary is usually round, as observed in *Bactrosaurus* and in most Hadrosauridae. In *Olorotitan arharensis* and *Tsintaosaurus spinorhinus*, on the other hand, the rostral margin of the predentary is nearly straight and forms right angles with the lateral sides of the bone.
30. Dentary crowns broad with a dominant ridge and secondary ridges (0), or miniaturized with or without faint secondary ridges (1).
31. Median carina of dentary teeth straight, (0) or sinuous (1).
32. Angle beween root and crown of dentary teeth more (0), or less (1) than 130°.
33. A maximum of 7 (0), or a minimum of 8 (1) sacral vertebrae.
34. Coracoid hook small and pointed ventrally (0), or prominent and pointed cranioventrally (1).
35. Deltopectoral crest of the humerus moderately (0), or strongly (1) developed, extending down below midshaft.
36. Antitrochanter of ilium absent or poorly developed (0), or prominent (1).
37. Ischial peduncle of ilium as a single large knob (0), or formed by two small protrusions separated by a shallow depression (1).
38. Distal end of ilium forming a moderately expanded knob (0), hypertrophied and footed (1), or tapering distally (2)—Character treated as unordered.
39. Distal head of fibula moderately expanded into the shape of a ball (0), or greatly expanded and club-shaped (1).
40. Cranial ascending process of astragalus laterally skewed (0), or equilateral in shape (1).

Appendix 2

Character—taxon matrix for phylogenetic analysis of *Amurosaurus riabinini*. ? = missing data; 0–2 = character states (see Appendix 1); v = variable within the taxon.

Bactrosaurus	00000 0000? 00000 00000 00000 00000 00000 00000
Hadrosaurinae	0000v 00101 01001 00010 11011 11101 01110 11200
Tsintaosaurus	01101 0???? ???21 10011 10111 11111 10111 11100
Jaxartosaurus	01111 0???? ????1 100?? ????? ????? ????? ?????
Amurosaurus	01111 0???? ????1 10111 10111 111?1 10?11 11?00
Parasaurolophus	11121 21000 10001 11111 10111 11101 10111 11111
Charonosaurus	11121 1???? ????1 11111 10111 111?1 10111 11111
Lambeosaurus	01111 11010 10101 10111 10111 11101 10111 11100
Corythosaurus	01111 11010 10111 10111 10111 11101 10111 11100
Hypacrosaurus	01111 11010 10111 10111 10111 11101 10111 11100
Olorotitan	01111 11010 10?11 1??12 10111 11111 10111 11100